Carcinogenesis vol.30 no.2 pp.214–221, 2009
doi:10.1093/carcin/bgn268
Advance Access publication November 26, 2008

Genome-wide DNA methylation profiles in both precancerous conditions and clear cell renal cell carcinomas are correlated with malignant potential and patient outcome

Eri Arai, Saori Ushijima, Hiroyuki Fujimoto[1], Fumie Hosoda[2], Tatsuhiro Shibata[2], Tadashi Kondo[3], Sana Yokoi[4], Issei Imoto[4], Johji Inazawa[4], Setsuo Hirohashi and Yae Kanai*

Pathology Division, National Cancer Center Research Institute, 5-1-1 Tsukiji, Chuo-ku, Tokyo 104-0045, Japan, [1]Urology Division, National Cancer Center Hospital, Tokyo 104-0045, Japan, [2]Cancer Genomics Project and [3]Proteome Bioinformatics Project, National Cancer Center Research Institute, Tokyo 104-0045, Japan and [4]Department of Molecular Cytogenetics, Medical Research Institute and School of Biomedical Science, Tokyo Medical and Dental University, Tokyo 113-8510, Japan

*To whom correspondence should be addressed. Tel: +81 3 3542 2511; Fax: +81 3 3248 2463;
Email: ykanai@ncc.go.jp

To clarify genome-wide DNA methylation profiles during multistage renal carcinogenesis, bacterial artificial chromosome array-based methylated CpG island amplification (BAMCA) was performed. Non-cancerous renal cortex tissue obtained from patients with clear cell renal cell carcinomas (RCCs) (N) was at the precancerous stage where DNA hypomethylation and DNA hypermethylation on multiple bacterial artificial chromosome (BAC) clones were observed. By unsupervised hierarchical clustering analysis based on BAMCA data for their N, 51 patients with clear cell RCCs were clustered into two subclasses, Clusters A_N ($n = 46$) and B_N ($n = 5$). Clinicopathologically aggressive clear cell RCCs were accumulated in Cluster B_N, and the overall survival rate of patients in Cluster B_N was significantly lower than that of patients in Cluster A_N. By unsupervised hierarchical clustering analysis based on BAMCA data for their RCCs, 51 patients were clustered into two subclasses, Clusters A_T ($n = 43$) and B_T ($n = 8$). Clinicopathologically aggressive clear cell RCCs were accumulated in Cluster B_T, and the overall survival rate of patients in Cluster B_T was significantly lower than that of patients in Cluster A_T. Multivariate analysis revealed that belonging to Cluster B_T was an independent predictor of recurrence. Cluster B_N was completely included in Cluster B_T, and the majority of the BAC clones that significantly discriminated Cluster B_N from Cluster A_N also discriminated Cluster B_T from Cluster A_T. In individual patients, DNA methylation status in N was basically inherited by the corresponding clear cell RCC. DNA methylation alterations in the precancerous stage may generate more malignant clear cell RCCs and determine patient outcome.

Introduction

It is known that DNA hypomethylation results in chromosomal instability as a result of changes in chromatin structure and that DNA hypermethylation of CpG islands silences tumor-related genes in cooperation with histone modification in human cancers (1–5). Accumulating evidence suggests that alterations of DNA methylation are involved even in the early and the precancerous stages (6,7). On the other hand, in patients with cancers, aberrant DNA methylation is significantly associated with poorer tumor differentiation, tumor aggressiveness and poor prognosis (6,7). Therefore, alterations of DNA methylation may play a significant role in multistage carcinogenesis and can become an indicator for carcinogenetic risk estimation and a biological predictor of poor prognosis in patients with cancers. Recently developed array-based technology for accessing genome-wide DNA methylation status (8–10) is now mainly used to identify tumor-related genes silenced by DNA methylation in human cancers. Subclassification of cancers based on DNA methylation status, which may reflect the distinct epigenetic pathways of carcinogenesis, and DNA methylation profiles, which could become the optimum indicator for carcinogenetic risk estimation and prediction of patient outcome, should be further explored in each organ using array-based approaches.

With respect to renal carcinogenesis, we have reported that accumulation of DNA methylation on C-type CpG islands occurs in a cancer-specific but not age-dependent manner (11), even in non-cancerous renal tissue samples obtained from patients with clear cell renal cell carcinomas (RCCs) (6,7,12). Although precancerous conditions in the kidney have been rarely described, from the viewpoint of altered DNA methylation, non-cancerous renal tissues obtained from patients with clear cell RCCs are considered to already be at the precancerous stage in spite of showing no remarkable histological changes and lacking association with chronic inflammation and persistent infection with viruses or other pathogenic microorganisms. Surprisingly, accumulation of DNA methylation on C-type CpG islands in such non-cancerous renal tissues has been shown to be significantly correlated with higher histological grades of the corresponding clear cell RCCs developing in individual patients (6,7,12). However, since in the previous study we examined DNA methylation status on only a restricted number of CpG islands (12), we were unable to conclude that genome-wide DNA methylation alterations in precancerous conditions generate more malignant RCCs. In the previous study, accumulation of DNA methylation on C-type CpG islands in clear cell RCCs themselves was significantly correlated with tumor aggressiveness and poorer patient outcome (12). However, we were unable to conclude that the examined C-type CpG islands are the optimum prognostic indicator for patients with clear cell RCCs.

In this study, in order to clarify genome-wide DNA methylation profiles during multistage renal carcinogenesis, we performed bacterial artificial chromosome array-based methylated CpG island amplification (BAMCA) (13–15) using a microarray of 4361 bacterial artificial chromosome (BAC) clones (16) in normal renal cortex tissue samples, non-cancerous renal cortex tissue samples obtained from patients with clear cell RCC and the corresponding clear cell RCCs.

Abbreviations: BAC, bacterial artificial chromosome; BAMCA, bacterial artificial chromosome array-based methylated CpG island amplification; RCC, renal cell carcinoma; TNM, tumor–node–metastasis.

Materials and methods

Patients and tissue samples

Paired specimens of cancerous tissue (T1–T51) and corresponding non-cancerous renal cortex tissue showing no remarkable histological changes (N1–N51) were obtained from materials surgically resected from 51 patients (RCC1–RCC 51) with primary clear cell RCC. These patients did not receive preoperative treatment and underwent nephrectomy in 1999–2006 at the National Cancer Center Hospital, Tokyo, Japan. There were 34 men and 17 women with a mean (±SD) age of 59 ± 10 years (range 31–81 years). Histological diagnosis was made in accordance with the World Health Organization classification (17). All the tumors were graded on the basis of

previously described criteria (18) and classified according to the pathological tumor–node–metastasis (TNM) classification (19). The criteria for macroscopic configuration of RCC (12) followed those established for hepatocellular carcinoma: type 3 (contiguous multinodular type) hepatocellular carcinomas show poorer histological differentiation and a higher incidence of intrahepatic metastasis than type 1 (single nodular type) and type 2 (single nodular type with extranodular growth) hepatocellular carcinomas (20). The presence or absence of vascular involvement was examined microscopically on slides stained with hematoxylin–eosin and elastica van Gieson. The presence or absence of tumor thrombi in the main trunk of the renal vein was examined macroscopically. RCC is usually encapsulated by a fibrous capsule and well demarcated and hardly ever contains fibrous stroma between cancer cells (panel T in Figure 1A). Therefore, we were able to obtain cancer cells of high purity from surgical specimens, avoiding contamination with both non-cancerous epithelial cells and stromal cells.

For comparison, eight normal renal cortex tissue samples (C1–C8) were obtained from materials surgically resected from eight patients without any primary renal tumor. These patients included five men and three women with a mean (±SD) age of 61 ± 12 years (range 47–81 years). Six of these patients underwent nephroureterectomy for urothelial carcinomas of the ureter, and the other two patients underwent nephrectomy with resection of retroperitoneal sarcoma around the kidney.

High-molecular weight DNA from these fresh frozen tissue samples was extracted using phenol–chloroform, followed by dialysis. Because DNA methylation status is known to be organ specific (21), the reference DNA for analysis of the developmental stages of clear cell RCC should be obtained from the renal cortex and not from other organs or peripheral blood. Therefore, a mixture of normal renal cortex tissue DNA obtained from six male patients (C9–C14) without any primary renal tumor was used as a reference for analyses of male test DNA samples, and a mixture of normal renal cortex tissue DNA obtained from three female patients (C15–C17) without any primary renal tumor was used as a reference for analyses of female test DNA samples.

This study was approved by the Ethics Committee of the National Cancer Center, Tokyo, Japan.

BAMCA

DNA methylation status was analyzed by BAMCA using a custom-made array (MCG Whole Genome Array-4500) harboring 4361 BAC clones throughout chromosomes 1–22 and X and Y (16), as described previously (13–15). Briefly, 5 μg aliquots of test or reference DNA were first digested with 100 U of methylation-sensitive restriction enzyme SmaI and subsequently with 20 U of methylation-insensitive XmaI. Adapters were ligated to XmaI-digested sticky ends, and polymerase chain reaction was performed with an adapter primer set. Test and reference polymerase chain reaction

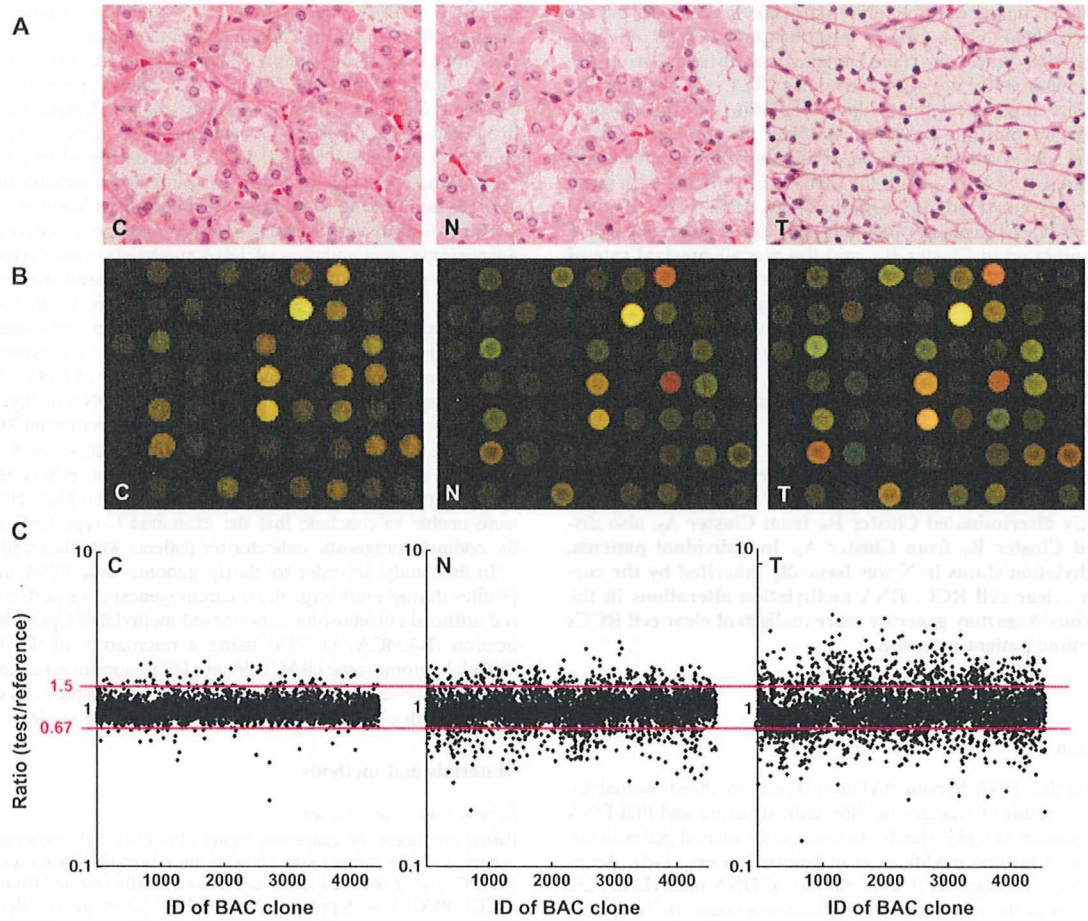

Fig. 1. DNA methylation alterations during multistage renal carcinogenesis. (**A**) Microscopic view of normal renal cortex tissue obtained from a patient without any primary renal tumor (C), non-cancerous renal cortex tissue obtained from a patient with clear cell RCC (N) and clear cell RCC (T). N shows no remarkable histological changes compared with C, i.e. no cytological or structural atypia is evident in N. Since T hardly ever contains fibrous stroma between cancer cells, we were able to obtain cancer cells of high purity, avoiding contamination with stromal cells. Hematoxylin–eosin staining. Original magnification ×20. (**B**) Scanned array images yielded by BAMCA in C, N and T. Test and reference DNA labeled with Cy3 and Cy5 was cohybridized, respectively. (**C**) Scattergrams of the signal ratios (test signal:reference signal) yielded by BAMCA in C, N and T. In all eight C samples (C1–C8), the signal ratios of 97% of BAC clones were between 0.67 and 1.5 (red bars). Therefore, in N and T, DNA methylation status corresponding to a signal ratio of <0.67 and >1.5 was defined as DNA hypomethylation and DNA hypermethylation on each BAC clone compared with C, respectively. Even though N did not show any remarkable histological changes compared with C [panels C and N in (A)], many BAC clones showed DNA hypomethylation or hypermethylation. In T, more BAC clones showed DNA hypomethylation or hypermethylation, and the degree of DNA hypomethylation and hypermethylation, i.e. deviation of the signal ratio from 0.67 or 1.5, was increased in comparison with N.

products were labeled by random priming with Cy3- and Cy5-dCTP (GE Healthcare, Buckinghamshire, UK), respectively, using a BioPrime array CGH genomic labeling system (Invitrogen, Carlsbad, CA) and precipitated together with ethanol in the presence of Cot-I DNA. The mixture was applied to array slides and incubated at 43°C for 72 h. Arrays were scanned with a GenePix Personal 4100A (Axon Instruments, Foster City, CA) and analyzed using GenePix Pro 5.0 imaging software (Axon Instruments) and Acue 2 software (Mitsui Knowledge Industry, Tokyo, Japan). The signal ratios were normalized in each sample to make the mean signal ratios of all BAC clones 1.0.

Statistics

Differences in the average number of BAC clones that showed DNA methylation alterations (DNA hypomethylation and hypermethylation) between non-cancerous renal cortex tissue samples obtained from patients with clear cell RCCs, and the clear cell RCCs themselves, were analyzed using the Mann–Whitney *U*-test. Differences at $P < 0.05$ were considered significant. Two-dimensional unsupervised hierarchical clustering analysis of the patients with clear cell RCCs and the BAC clones based on the signal ratios (test signal: reference signal) obtained by BAMCA in non-cancerous renal cortex tissue samples and those in clear cell RCCs were performed using the Expressionist software program (Gene Data, Basel, Switzerland). Correlations between the subclassification of patients with clear cell RCCs yielded by the unsupervised hierarchical clustering based on DNA methylation status of non-cancerous renal cortex tissue samples (Clusters A_N and B_N) and clinicopathological parameters of the corresponding clear cell RCCs were analyzed using chi-square test. Correlations between the subclassification of patients yielded by the unsupervised hierarchical clustering based on DNA methylation status in clear cell RCCs (Clusters A_T and B_T) and clinicopathological parameters of the RCCs themselves were analyzed using chi-square test. Survival curves of patients belonging to Clusters A_N versus B_N and Clusters A_T versus B_T were calculated by the Kaplan–Meier method, and the differences were compared by the Log-rank test. The Cox proportional hazards multivariate model was used to examine the prognostic impact of the subclassification of patients based on the DNA methylation status of their clear cell RCCs (Clusters A_T and B_T), histological grade, macroscopic configuration, vascular involvement and renal vein tumor thrombi. Differences at $P < 0.05$ were considered significant. BAC clones whose signal ratios were significantly different between Clusters A_N and B_N and Clusters A_T and B_T were each identified by Wilcoxon test ($P < 0.01$).

Results

DNA methylation alterations in samples of both cancerous and non-cancerous renal cortex tissue obtained from patients with clear cell RCCs

Figure 1B and C shows examples of scanned array images and scattergrams of the signal ratios (test signal:reference signal), respectively, for normal renal cortex tissue from a patient without any primary renal tumor and both non-cancerous renal cortex tissue and cancerous tissue from a patient with clear cell RCC. In all normal renal cortex tissue samples (C1–C8), the signal ratios of 97% of the BAC clones were between 0.67 and 1.5 (red bars in Figure 1C). Therefore, in non-cancerous renal cortex tissue obtained from patients with clear cell RCCs and the clear cell RCCs themselves, DNA methylation status corresponding to a signal ratio of <0.67 and >1.5 was defined as DNA hypomethylation and DNA hypermethylation of each BAC clone compared with normal renal cortex tissue, respectively. In samples of non-cancerous renal cortex tissue obtained from patients with clear cell RCCs (N1–N51), many BAC clones showed DNA hypomethylation or DNA hypermethylation (panel N of Figure 1C). In clear cell RCCs themselves (T1–T51), more BAC clones showed DNA hypomethylation or DNA hypermethylation, and the degree of DNA hypomethylation and DNA hypermethylation, i.e. deviation of the signal ratio from 0.67 or 1.5, was increased in comparison with non-cancerous renal cortex tissue samples obtained from patients with clear cell RCCs (panel T of Figure 1C). The average number of BAC clones showing DNA hypomethylation increased significantly from non-cancerous renal cortex tissue samples obtained from patients with clear cell RCCs (93 ± 75) to clear cell RCCs (142 ± 74, $P = 0.0002$). The average number of BAC clones showing DNA hypermethylation also increased significantly in a similar manner (83 ± 73–123 ± 786, $P = 0.004$).

Unsupervised hierarchical clustering of patients with clear cell RCCs based on DNA methylation status of non-cancerous renal cortex tissue samples

By two-dimensional unsupervised hierarchical clustering analysis based on BAMCA data (signal ratios) for non-cancerous renal cortex tissue samples, the 51 patients with clear cell RCCs were clustered into two subclasses, Clusters A_N and B_N, which contained 46 and 5 patients, respectively (Figure 2A).

Table IA shows the clinicopathological parameters of clear cell RCCs of patients belonging to Clusters A_N and B_N. The corresponding clear cell RCCs of patients in Cluster B_N showed more frequent macroscopically evident multinodular (type 3) growth, vascular involvement and renal vein tumor thrombi and showed higher pathological TNM stages than those in Cluster A_N. Figure 2B shows the Kaplan–Meier survival curves of patients belonging to Clusters A_N and B_N. The period covered ranged from 88 to 2801 days (mean, 1679 days). Three (60%) of the patients in Cluster B_N died of recurrent RCC, whereas only one (2%) of the patients in Cluster A_N died. The overall survival rate of patients in Cluster B_N was significantly lower than that of patients in Cluster A_N (Figure 2B).

Although Cluster A_N was divided into three subclusters, A_{N1} ($n = 3$), A_{N2} ($n = 19$) and A_{N3} ($n = 24$) (Figure 2A), there were no significant correlations between these subclusters and any of the clinicopathological parameters examined (data not shown). Even when unsupervised hierarchical clustering was performed separately, based not on signal ratios but on the presence or absence of DNA hypomethylation and the presence or absence of DNA hypermethylation, the majority of patients in Cluster B_N were clustered into the same subclass (supplementary Figure S1A and B is available at *Carcinogenesis* Online).

Wilcoxon test ($P < 0.01$) revealed that the signal ratios of 1143 BAC clones in non-cancerous renal cortex tissue differed significantly between Clusters A_N and B_N: e.g. patients belonging to Cluster B_N were completely discriminated from patients in Cluster A_N by the DNA methylation status of samples of non-cancerous renal cortex tissue for representative BAC clones (Cluster A_N versus Cluster B_N in Figure 3A) out of the 1143 BAC clones.

Unsupervised hierarchical clustering based on DNA methylation status of clear cell RCCs

Two-dimensional unsupervised hierarchical clustering analysis based on BAMCA data (signal ratios) for clear cell RCCs was able to group 51 patients into two subclasses, Clusters A_T and B_T, which contained 43 and eight patients, respectively (Figure 2C).

Table IB shows the clinicopathological parameters of clear cell RCCs of patients belonging to Clusters A_T and B_T. Clear cell RCCs in Cluster B_T showed more frequent vascular involvement and renal vein tumor thrombi and showed higher pathological TNM stages than those in Cluster A_T. Figure 2D shows the Kaplan–Meier survival curves of patients belonging to Clusters A_T and B_T. Three (37.5%) of the patients in Cluster B_T died due to recurrent RCCs, whereas only one (2.3%) of the patients in Cluster A_T died. The overall survival rate of patients in Cluster B_T was significantly lower than that of patients in Cluster A_T (Figure 2D). Multivariate analysis revealed that our clustering was a predictor of recurrence and was independent of histological grade, macroscopic configuration, vascular involvement and renal vein tumor thrombi (Table II).

Although Cluster A_T was divided into four subclusters, A_{T1} ($n = 8$), A_{T2} ($n = 12$), A_{T3} ($n = 13$) and A_{T4} ($n = 10$) (Figure 2B), there were no significant correlations between these subclusters and any of the clinicopathological parameters examined (data not shown). Even when unsupervised hierarchical clustering was performed separately, based not on signal ratios but on the presence or absence of DNA hypomethylation and the presence or absence of DNA hypermethylation, the majority of patients in Cluster B_T were clustered into the same subclass (supplementary Figure S1C and D is available at *Carcinogenesis* Online).

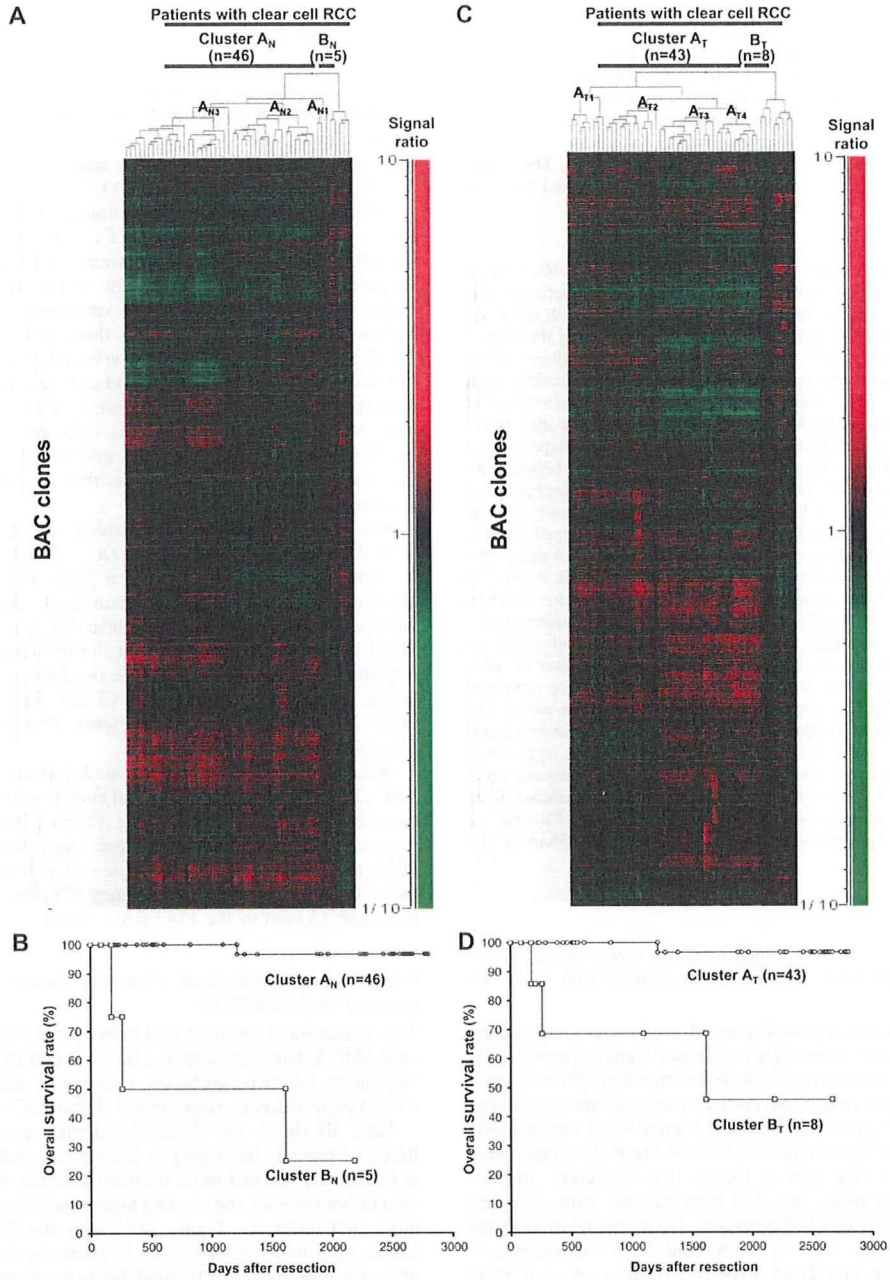

Fig. 2. Two-dimensional unsupervised hierarchical clustering analysis based on BAMCA data (signal ratios) in non-cancerous renal cortex tissue samples showing no remarkable histological changes (A) and clear cell RCCs (C) and Kaplan–Meier survival curves of patients with clear cell RCCs (B and D). (**A**) Fifty-one patients with clear cell RCC were hierarchically clustered into two subclasses, Clusters A_N (n = 46) and B_N (n = 5), based on DNA methylation status of their non-cancerous renal cortex tissue samples. DNA hypomethylation, normomethylation (DNA methylation status corresponding to a signal ratio of between 0.67 and 1.5) and hypermethylation on each BAC clone are shown in green, black and red, respectively. The signal ratio is shown in the color range maps. The cluster trees for patients and BAC clones are shown at the top and left of the panel, respectively. (**B**) The overall survival rate of patients in Cluster B_N (square) defined on the basis of DNA methylation status in their non-cancerous renal cortex tissue samples was significantly lower than that of patients in Cluster A_N (circle) (P = 0.0000000613, Log-rank test). (**C**) Fifty-one patients were hierarchically clustered into two subclasses, Clusters A_T (n = 43) and B_T (n = 8), based on the DNA methylation status of their clear cell RCCs. (**D**) The overall survival rate of patients in Cluster B_T (square) defined on the basis of DNA methylation status in their clear cell RCCs was significantly lower than that of patients in Cluster A_T (circle) (P = 0.0000413, Log-rank test).

Wilcoxon test ($P < 0.01$) revealed that the signal ratios of 1111 BAC clones in clear cell RCCs were differed significantly between Clusters A_T and B_T. In particular, patients belonging to Cluster B_T were completely discriminated from patients belonging to Cluster A_T based on the DNA methylation status of 14 BAC clones (Cluster A_T versus Cluster B_T in Figure 3A). In other words, DNA methylation status of the 14 BAC clones was able to determine whether or not patients in this cohort belonged to Cluster B_T, a significant prognostic indicator, with a sensitivity and specificity of 100% using the cutoff values shown in Figure 3A and supplementary Table

Table I. Correlation between the subclassification of patients based on DNA methylation status and the clinicopathological parameters of clear cell RCCs

(A) Clusters A_N and B_N based on DNA methylation status in non-cancerous renal cortex tissue samples				
Clinicopathalogical parameters of the corresponding clear cell RCCs developing in individual patients		Patients with clear cell RCCs		P^a
		Cluster A_N (n = 46)	Cluster B_N (n = 5)	
Macroscopic finding	Type 1	26	1	0.0248
	Type 2	10	0	
	Type 3	10	4	
Vascular involvement	Negative	38	0	0.0005
	Positive	8	5	
Renal vein tumor thrombi	Negative	41	1	0.0017
	Positive	5	4	
Pathological TNM stage	Stage I	29	0	0.0195
	Stage II	1	0	
	Stage III	13	3	
	Stage IV	3	2	
(B) Clusters A_T and B_T based on DNA methylation status in clear cell RCCs				
Clinicopathalogical parameters of clear cell RCCs		Patients with clear cell RCCs		P^a
		Cluster A_T (n = 43)	Cluster B_T (n = 8)	
Macroscopic finding	Type 1	24	3	NS[b]
	Type 2	9	1	
	Type 3	10	4	
Vascular involvement	Negative	35	3	0.0297
	Positive	8	5	
Renal vein tumor thrombi	Negative	38	4	0.0349
	Positive	5	4	
Pathological TNM stage	Stage I	27	2	0.0263
	Stage II	1	0	
	Stage III	13	3	
	Stage IV	2	3	

[a]Chi-square test.
[b]Not significant.

SI (available at *Carcinogenesis* Online). DNA methylation status of the 70 BAC clones, including the above 14 BAC clones, was able to determine whether or not the patients in this cohort belonged to Cluster B_T, with a sensitivity of 100% and a specificity of 90 or >90%, using the cutoff values shown in supplementary Table SI (available at *Carcinogenesis* Online).

Comparison between DNA methylation profiles of non-cancerous renal tissue and those of corresponding clear cell RCC

Patients RCC1–RCC5 and patients RCC1–RCC8 were identified as belonging to Clusters B_N and B_T, respectively, by unsupervised hierarchical clustering based on BAMCA data for non-cancerous renal cortex tissue samples and clear cell RCCs. Namely, Cluster B_N (n = 5) was completely included in Cluster B_T (n = 8). The 724 BAC clones, the majority of the 1143 BAC clones significantly discriminating Cluster B_N from Cluster A_N, also discriminated Cluster B_T from Cluster A_T (Wilcoxon test, $P < 0.01$). In 311 of the 724 BAC clones, where the average signal ratio of Cluster B_N was higher than that of Cluster A_N, the average signal ratio of Cluster B_T was also higher than that of Cluster A_T without exception (Figure 3A). In 413 of the 724 BAC clones, where the average signal ratio of Cluster B_N was lower than that of Cluster A_N, the average signal ratio of Cluster B_T was also lower than that of Cluster A_T without exception (Figure 3A). Figure 3B shows the signal ratios of non-cancerous renal cortex tissue samples and clear cell RCCs for all 51 patients for a representative BAC clone (RP11-44F3). In individual patients, DNA methylation status in the non-cancerous renal cortex tissue was basically inherited by the corresponding clear cell RCC (Figure 3B).

Discussion

Many researchers in this field use arrays in which the promoter regions are enriched as probes to identify the genes methylated in cancer cells (8–10). However, the promoter regions of specific genes are not the only target of DNA methylation alterations in human cancers. DNA methylation status in genomic regions not directly participating in gene silencing, such as the edges of CpG islands, may be altered at the precancerous stage before the alterations of the promoter regions themselves occur (22). Genomic regions in which DNA hypomethylation affects chromosomal instability may not be contained in promoter arrays. Moreover, aberrant DNA methylation of large regions of chromosomes, which are regulated in a coordinated manner in human cancers due to a process of long-range epigenetic silencing, has recently attracted attention (23). Therefore, we used a custom-made BAC array (16) that may be suitable, not for focusing on specific promoter regions or individual CpG sites but for overviewing the DNA methylation status of individual large regions among all chromosomes and for subclassifying cancers by hierarchical clustering.

With respect to renal carcinogenesis, several studies of DNA methylation profiles of genes involved in specific signal pathways in clear cell RCCs, such as the p53-signaling (24) and Wnt-signaling (25) pathways, have been performed. However, to our knowledge, there have been no published data on DNA methylation profiles for all chromosomes in clear cell RCCs revealed by array-based technology. In our previous study, we showed that samples of non-cancerous renal cortex tissue from patients with clear cell RCC were already at the precancerous stage with accumulation of DNA methylation on C-type CpG islands, in spite of an absence of marked histological changes (6,7,12). In the present study, genome-wide DNA methylation alterations (both hypomethylation and hypermethylation) in samples of non-cancerous renal cortex tissue from patients with clear cell RCC were confirmed by BAMCA (panel N of Figure 1B and C). We then performed unsupervised hierarchical clustering analysis based on the genome-wide DNA methylation status of the non-cancerous renal cortex tissue samples, and as a result, 51 patients were subclassified into Clusters A_N and B_N. Corresponding clear cell RCCs showing multinodular growth, vascular involvement, renal vein tumor thrombi and higher pathological TNM stages were found to be accumulated in Cluster B_N. Although subclassification of precancerous tissue by unsupervised hierarchical clustering analysis on the basis of genome-wide DNA methylation profiles has never been performed for specific organs, our Clusters A_N and B_N can be considered clinicopathologically valid.

The significant correlation between genome-wide DNA methylation profiles of samples of non-cancerous renal cortex tissue and

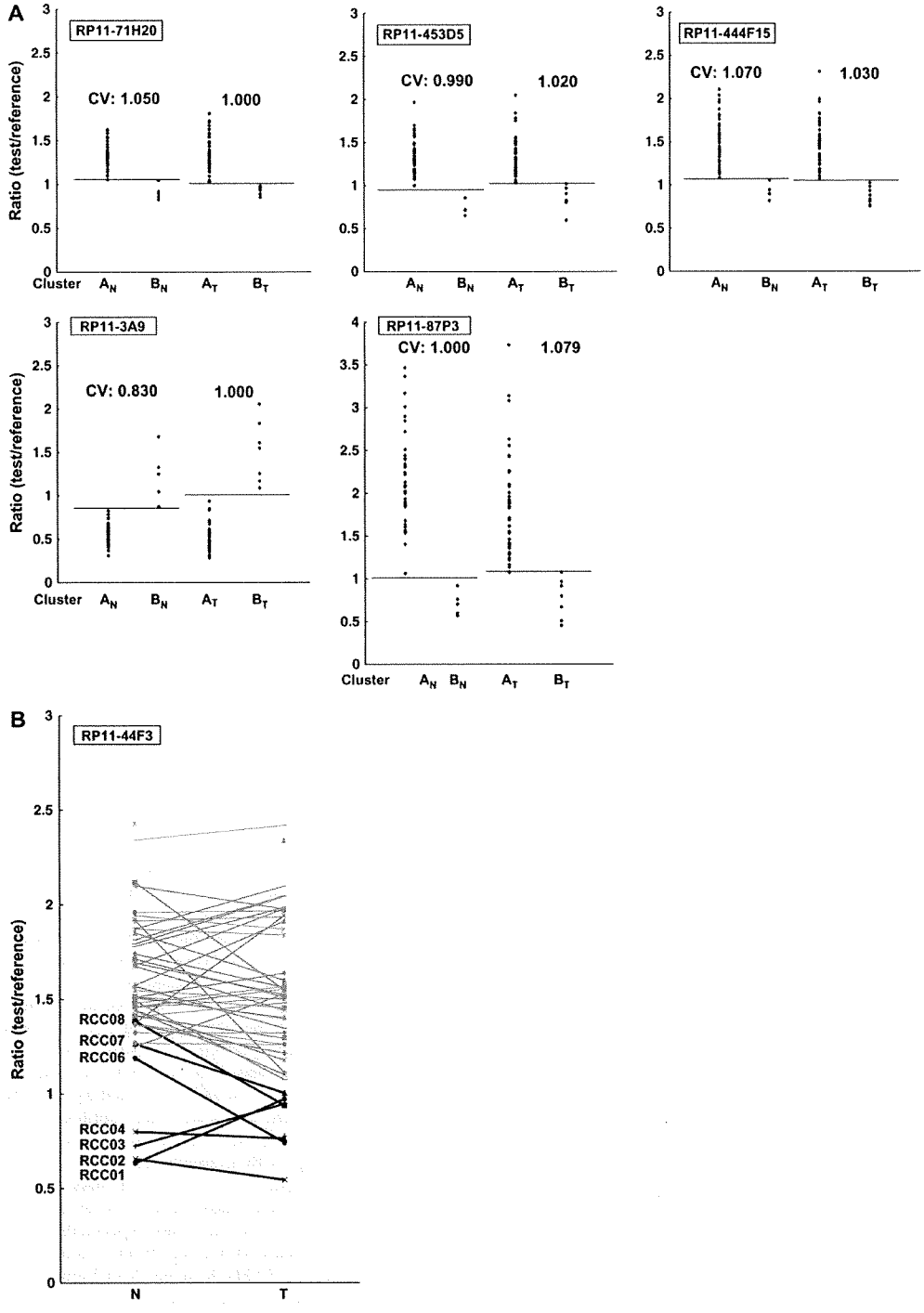

Fig. 3. (**A**) Scattergrams of the signal ratios in non-cancerous renal cortex tissue samples (Cluster A_N versus Cluster B_N) and in clear cell RCCs (Cluster A_T versus Cluster B_T) on representative BAC clones, RP11-71H20, RP11-453D5, RP11-444F15, RP11-3A9 and RP11-87P3. Using the cutoff values (CVs) described in each panel, patients belonging to Cluster B_N were completely discriminated from patients in Cluster A_N based on the DNA methylation status of non-cancerous renal cortex tissue samples. Using the cutoff value described in each panel, patients belonging to Cluster B_T were completely discriminated from patients in Cluster A_T based on the DNA methylation status of the clear cell RCCs. When the signal ratios of Cluster B_N were lower than those of Cluster A_N, the signal ratios of Cluster B_T were also lower than those of Cluster A_T (RP11-71H20, RP11-453D5, RP11-444F15 and RP11-87P3). When the signal ratios of Cluster B_N were higher than those of Cluster A_N, the signal ratios of Cluster B_T were also higher than those in Cluster A_T (RP11-3A9). (**B**) The signal ratios of non-cancerous renal cortex tissue (N) and clear cell RCC (T) for all 51 patients on a representative BAC clone (RP11-44F3). DNA methylation status in N was basically inherited in the corresponding T developing in the individual patient. Gray bar, patients belonging to Cluster A_T; black bar, patients belonging to Cluster B_T. The case numbers of patients belonging to Cluster B_T (RCC1–RCC8) are also shown on the left side. Patients RCC6–RCC8 did not belong to Cluster B_N, but later gained the same DNA methylation profiles as those of patients RCC1–RCC5 during the development of T from N, and joined Cluster B_T.

Table II. Multivariate analysis of the clinicopathological parameters and the subclassification (Clusters A_T and B_T) based on DNA methylation status of cancerous tissue samples as predictors of recurrence

Parameters	Hazard ratio (95% CI)	χ^2	*P* value
Histological grade			
Grade 1, 2 or 3	1 (Reference)		
Grade 4	118.582 (5.186–2711.249)	8.947	0.0028
Macroscopic configuration			
Type 1	1 (Reference)		
Type 2	5.309 (0.689–40.887)	2.570	0.1089
Type 3	0.820 (0.061–11.005)	0.022	0.8808
Vascular involvement			
Negative	1 (Reference)		
Positive	1.434 (0.098–20.932)	0.070	0.7920
Renal vein tumor thrombi			
Negative	1 (Reference)		
Positive	8.780 (0.429–179.734)	1.990	0.1584
Subclassification based on DNA methylation status			
Cluster A_T	1 (Reference)		
Cluster B_T	8.317 (1.100–62.901)	4.211	0.0402

CI, confidence interval.

aggressiveness of cancers developing in individual patients indicated that it may be possible to estimate the future risk of developing more malignant cancers based on genome-wide DNA methylation status at the precancerous stage. Although kidney biopsy sampling for screening of healthy individuals is not clinically feasible because of its invasive nature, carcinogenetic risk estimation using urine, sputum and other body fluid samples may be a promising approach if optimal indicators can be identified by genome-wide DNA methylation profiling at the precancerous stage in the urinary tract, lung and other organs. Patients belonging to Cluster B_N showed poorer outcome than those in Cluster A_N, indicating that even patient outcome is determined by DNA methylation status at the precancerous stage.

Although altered DNA methylation on several CpG islands has been reported separately in RCCs (26–28), subclassification of clear cell RCCs, which may reflect the distinct epigenetic pathways of carcinogenesis, has never been established on the basis of genome-wide DNA methylation profiling. Since clear cell RCCs showing a higher incidence of vascular involvement, renal vein tumor thrombi and higher pathological TNM stages were accumulated in Cluster B_T, our Clusters A_T and B_T can be considered clinicopathologically valid. In our previous studies, we examined DNA methylation status on CpG islands for the *p16*, *hMLH 1*, *VHL* and *THBS 1* genes, and the methylated in tumor-1, -2, -12, -25 and -31 clones were examined in the same 51 clear cell RCCs (12,29). Correlations between DNA methylation status on each CpG island and our clustering are summarized in supplementary Table SII (available at *Carcinogenesis* Online). The average number of methylated CpG islands was significantly higher in Cluster B_T (2.75 ± 1.67) than in Cluster A_T (1.54 ± 0.98, $P = 0.01867318$). Patients were considered to be positive for the CpG island methylator phenotype when DNA methylation was seen on three or more examined CpG islands, based on previously described criteria (11). The frequency of CpG island methylator phenotype in Cluster B_T (62.5%) was significantly higher than that in Cluster A_T (16%, $P = 0.0174969$). Genome-wide DNA methylation alterations consisting of both hypomethylation and hypermethylation of DNA revealed by BAMCA in Cluster B_T are associated with regional DNA hypermethylation on CpG islands and participate in malignant progression of clear cell RCCs. Moreover, patients belonging to Cluster B_T showed poorer outcome than those in Cluster A_T, indicating that prognostication of clear cell RCCs using DNA methylation status as an indicator is a promising approach.

Some RCCs relapse and metastasize to distant organs, even if resection has been considered complete (17,30). Recently, immunotherapy (31) and novel targeting agents (32) have been developed for treatment of RCC. However, unless relapsed or metastasized tumors are diagnosed early by close follow-up, the effectiveness of any therapy is very restricted. Therefore, to assist close follow-up of patients who have undergone nephrectomy and are still at risk of recurrence and metastasis, prognostic indicators have been explored. Multivariate analysis revealed that belonging to Cluster B_T was an independent predictor of recurrence. It is known that sarcomatoid RCCs with grade 4 atypia frequently show recurrence (18). However, patients with RCCs showing grade 1–3 atypia also suffer recurrence, and we cannot estimate the risk of recurrence of such RCCs based on known parameters. Belonging to Cluster B_T is advantageous even to patients with RCCs showing grade 1–3 atypia because it is a predictor of recurrence that is independent of histological grading. For clinical application, a combination of several BAC clones from the 70 that showed 100% sensitivity and 90 or >90% specificity (including 14 BAC clones showing 100% sensitivity and 100% specificity) can be of optimal prognostic value for patients with clear cell RCCs. Since a sufficient quantity of good-quality DNA can be obtained from each nephrectomy specimen, polymerase chain reaction-based analyses focusing on individual CpG sites are not always required. Array-based analysis that overviews aberrant DNA methylation of each BAC region is immediately applicable to routine laboratory examinations for prognostication after nephrectomy. We are currently attempting to prepare a mini-array harboring some of the 70 BAC clones. The reliability of such prognostication will need to be validated in a prospective study.

We have clarified that genome-wide DNA methylation profiles of non-cancerous renal cortex tissue are inherited by the corresponding clear cell RCC based on the following findings: (i) all patients belonging to Cluster B_N were included in Cluster B_T; (ii) a majority of the BAC clones characterizing Cluster B_N (724 BAC clones) also characterized Cluster B_T; (iii) DNA methylation status on such 724 BAC clones of non-cancerous renal cortex tissue in Cluster A_N was in accordance with that of clear cell RCCs in Cluster A_T and that of non-cancerous renal cortex tissue in Cluster B_N was in accordance with that of clear cell RCCs in Cluster B_T (Figure 3A) and (iv) DNA methylation status in non-cancerous renal cortex tissue basically corresponded to that in the matching clear cell RCC in each patient (Figure 3B).

Patients RCC6–RCC8 who belonged to Cluster B_T but not to Cluster B_N may later gain the DNA methylation profiles observed in patients RCC1–RCC5 during the establishment of clear cell RCCs (Figure 3B) and suffer from the same degree of tumor aggressiveness as patients RCC1–RCC5. Although alterations of DNA methylation are considered to be involved even in the precancerous stage in various organs (6,7,33–35), it has not yet been clarified for any organ whether DNA methylation status on only a restricted number of CpG islands is simply altered at such stages or whether genome-wide alterations of DNA methylation status have certain clinicopathological significance. The present unsupervised hierarchical clustering revealed for the first time that DNA methylation alterations in precancerous conditions, which may not occur randomly but are prone to further accumulation of genetic and epigenetic alterations, can generate more malignant cancers and even determine the ultimate patient outcome.

Supplementary material

Supplementary Figure S1 and Tables SI and SII can be found at http://carcin.oxfordjournals.org/

Funding

Grant-in-Aid for the Third Term Comprehensive 10-Year Strategy for Cancer Control from the Ministry of Health, Labor and Welfare of Japan; Grant-in-Aid for Cancer Research from the Ministry of Health, Labor and Welfare of Japan; New Energy and Industrial Technology Development Organization; Program for Promotion of Fundamental Studies in Health Sciences of the National Institute of Biomedical

Innovation. Funding to pay the Open Access publication charges for this article was provided by a Grant-in-Aid for the Third Term Comprehensive 10-Year Strategy for Cancer Control from the Ministry of Health, Labor and Welfare of Japan.

Acknowledgements

Conflict of Interest Statement: None declared.

References

1. Jones,P.A. *et al.* (2002) The fundamental role of epigenetic events in cancer. *Nat. Rev. Genet.*, **3**, 415–428.
2. Eden,A. *et al.* (2003) Chromosomal instability and tumors promoted by DNA hypomethylation. *Science*, **300**, 455.
3. Baylin,S.B. *et al.* (2006) Epigenetic gene silencing in cancer—a mechanism for early oncogenic pathway addiction? *Nat. Rev. Cancer*, **6**, 107–116.
4. Gronbaek,K. *et al.* (2007) Epigenetic changes in cancer. *APMIS*, **115**, 1039–1159.
5. Feinberg,A.P. (2007) Phenotypic plasticity and the epigenetics of human disease. *Nature*, **447**, 433–440.
6. Kanai,Y. *et al.* (2007) Alterations of DNA methylation associated with abnormalities of DNA methyltransferases in human cancers during transition from a precancerous to a malignant state. *Carcinogenesis*, **28**, 2434–2442.
7. Kanai,Y. (2008) Alterations of DNA methylation and clinicopathological diversity of human cancers. *Pathol. Int.*, **58**, 544–558.
8. Estecio,M.R. *et al.* (2007) High-throughput methylation profiling by MCA coupled to CpG island microarray. *Genome Res.*, **17**, 1529–1536.
9. Jacinto,F.V. *et al.* (2007) Discovery of epigenetically silenced genes by methylated DNA immunoprecipitation in colon cancer cells. *Cancer Res.*, **67**, 11481–11486.
10. Nielander,I. *et al.* (2007) Combining array-based approaches for the identification of candidate tumor suppressor loci in mature lymphoid neoplasms. *APMIS*, **115**, 1107–1134.
11. Toyota,M. *et al.* (1999) CpG island methylator phenotype in colorectal cancer. *Proc. Natl Acad. Sci. USA*, **96**, 8681–8686.
12. Arai,E. *et al.* (2006) Regional DNA hypermethylation and DNA methyltransferase (DNMT) 1 protein overexpression in both renal tumors and corresponding nontumorous renal tissues. *Int. J. Cancer*, **119**, 288–296.
13. Misawa,A. *et al.* (2005) Methylation-associated silencing of the nuclear receptor 1I2 gene in advanced-type neuroblastomas, identified by bacterial artificial chromosome array-based methylated CpG island amplification. *Cancer Res.*, **65**, 10233–10242.
14. Sugino,Y. *et al.* (2007) Epigenetic silencing of prostaglandin E receptor 2 (PTGER2) is associated with progression of neuroblastomas. *Oncogene*, **26**, 7401–7413.
15. Tanaka,K. *et al.* (2007) Frequent methylation-associated silencing of a candidate tumor-suppressor, CRABP1, in esophageal squamous-cell carcinoma. *Oncogene*, **26**, 6456–6468.
16. Inazawa,J. *et al.* (2004) Comparative genomic hybridization (CGH)-arrays pave the way for identification of novel cancer-related genes. *Cancer Sci.*, **95**, 559–563.
17. Eble,J.N. *et al.* (2004) *Renal Cell Carcinoma. World Health Organization Classification of Tumours. Pathology and Genetics. Tumours of the Urinary System and Male Genital Organs,* IARC Press, Lyon, 10–43.
18. Fuhrman,S.A. *et al.* (1982) Prognostic significance of morphologic parameters in renal cell carcinoma. *Am. J. Surg. Pathol.*, **6**, 655–663.
19. Sobin,L.H. *et al.* (2002) *International Union Against Cancer (UICC). TNM Classification of Malignant Tumors,* 6th edn. Wiley-Liss, New York, NY, 193–195.
20. Kanai,T. *et al.* (1987) Pathology of small hepatocellular carcinoma. A proposal for a new gross classification. *Cancer*, **60**, 810–819.
21. Illingworth,R. *et al.* (2008) A novel CpG island set identifies tissue-specific methylation at developmental gene loci. *PLoS Biol.*, **6**, e22.
22. Maekita,T. *et al.* (2006) High levels of aberrant DNA methylation in *Helicobacter pylori*-infected gastric mucosae and its possible association with gastric cancer risk. *Clin. Cancer Res.*, **12**, 989–995.
23. Frigola,J. *et al.* (2006) Epigenetic remodeling in colorectal cancer results in coordinate gene suppression across an entire chromosome band. *Nat. Genet.*, **38**, 540–549.
24. Christoph,F. *et al.* (2006) Promoter hypermethylation profile of kidney cancer with new proapoptotic p53 target genes and clinical implications. *Clin. Cancer Res.*, **12**, 5040–5046.
25. Urakami,S. *et al.* (2006) Wnt antagonist family genes as biomarkers for diagnosis, staging, and prognosis of renal cell carcinoma using tumor and serum DNA. *Clin. Cancer Res.*, **12**, 6989–6997.
26. Ibanez de Caceres,I. *et al.* (2006) Identification of novel target genes by an epigenetic reactivation screen of renal cancer. *Cancer Res.*, **66**, 5021–5028.
27. Costa,V.L. *et al.* (2007) Quantitative promoter methylation analysis of multiple cancer-related genes in renal cell tumors. *BMC Cancer*, **7**, 133.
28. Morris,M.R. *et al.* (2008) Functional epigenomics approach to identify methylated candidate tumour suppressor genes in renal cell carcinoma. *Br. J. Cancer*, **98**, 496–501.
29. Arai,E. *et al.* (2008) Genetic clustering of clear cell renal cell carcinoma based on array-CGH: its association with DNA methylation alteration and patient outcome. *Clin. Cancer Res.*, **14**, 5531–5539.
30. Jones,J. *et al.* (2007) Genomics of renal cell cancer: the biology behind and the therapy ahead. *Clin. Cancer Res.*, **13**, 685s–692s.
31. Guida,M. *et al.* (2007) Immunotherapy for metastatic renal cell carcinoma: is it a therapeutic option yet? *Ann. Oncol.*, **18** (suppl. 6), vi149–52.
32. Patel,P.H. *et al.* (2006) Targeting von Hippel-Lindau pathway in renal cell carcinoma. *Clin. Cancer Res.*, **12**, 7215–7520.
33. Kanai,Y. *et al.* (1996) Aberrant DNA methylation on chromosome 16 is an early event in hepatocarcinogenesis. *Jpn. J. Cancer Res.*, **87**, 1210–1217.
34. Eguchi,K. *et al.* (1997) DNA hypermethylation at the D17S5 locus in non-small cell lung cancers: its association with smoking history. *Cancer Res.*, **57**, 4913–4915.
35. Peng,D.F. *et al.* (2006) DNA methylation of multiple tumor-related genes in association with overexpression of DNA methyltransferase 1 (DNMT1) during multistage carcinogenesis of the pancreas. *Carcinogenesis*, **27**, 1160–1168.

Received September 1, 2008; revised November 12, 2008; accepted November 20, 2008

Int. J. Cancer: **125,** 2854–2862 (2009)

Genome-wide DNA methylation profiles in liver tissue at the precancerous stage and in hepatocellular carcinoma

Eri Arai[1], Saori Ushijima[1], Masahiro Gotoh[1], Hidenori Ojima[1], Tomoo Kosuge[2], Fumie Hosoda[3], Tatsuhiro Shibata[3], Tadashi Kondo[4], Sana Yokoi[5], Issei Imoto[5], Johji Inazawa[5], Setsuo Hirohashi[1] and Yae Kanai[1]*

[1]*Pathology Division, National Cancer Center Research Institute, Tokyo, Japan*
[2]*Hepatobiliary and Pancreatic Surgery Division, National Cancer Center Hospital, Tokyo, Japan*
[3]*Cancer Genomics Project, National Cancer Center Research Institute, Tokyo, Japan*
[4]*Proteome Bioinformatics Project, National Cancer Center Research Institute, Tokyo, Japan*
[5]*Department of Molecular Cytogenetics, Medical Research Institute and School of Biomedical Science, Tokyo Medical and Dental University, Tokyo, Japan*

To clarify genome-wide DNA methylation profiles during hepatocarcinogenesis, bacterial artificial chromosome (BAC) array-based methylated CpG island amplification was performed on 126 tissue samples. The average numbers of BAC clones showing DNA hypo- or hypermethylation increased from noncancerous liver tissue obtained from patients with hepatocellular carcinomas (HCCs) (N) to HCCs. N appeared to be at the precancerous stage, showing DNA methylation alterations that were correlated with the future development of HCC. Using Wilcoxon test, 25 BAC clones, whose DNA methylation status was inherited by HCCs from N and were able to discriminate 15 N samples from 10 samples of normal liver tissue obtained from patients without HCCs (C) with 100% sensitivity and specificity, were identified. The criteria using the 25 BAC clones were able to discriminate 24 additional N samples from 26 C samples in the validation set with 95.8% sensitivity and 96.2% specificity. Using Wilcoxon test, 41 BAC clones, whose DNA methylation status was able to discriminate patients who survived more than 4 years after hepatectomy from patients who suffered recurrence within 6 months and died within a year after hepatectomy, were identified. The DNA methylation status of the 41 BAC clones was correlated with the cancer-free and overall survival rates of patients with HCC. Multivariate analysis revealed that satisfying the criteria using the 41 BAC clones was an independent predictor of overall outcome. Genome-wide alterations of DNA methylation may participate in hepatocarcinogenesis from the precancerous stage, and DNA methylation profiling may provide optimal indicators for carcinogenetic risk estimation and prognostication.

Key words: bacterial artificial chromosome array-based methylated CpG island amplification; hepatocellular carcinoma; multistage carcinogenesis; precancerous condition; prognostication

Alteration of DNA methylation is one of the most consistent epigenetic changes in human cancers.[1,2] It is known that DNA hypomethylation results in chromosomal instability as a result of changes in the chromatin structure, and that DNA hypermethylation of CpG islands silences tumor-related genes in cooperation with histone modification in human cancers.[3,4]

With respect to hepatocarcinogenesis, we have shown that alterations of DNA methylation at multiple chromosomal loci can be detected even in noncancerous liver tissue showing chronic hepatitis or cirrhosis, which are widely considered to be precancerous conditions, but not in normal liver tissue, using classical Southern blotting analysis.[5] This was one of the earliest reports of alterations of DNA methylation at the precancerous stage. Multiple tumor-related genes, such as the *E-cadherin*[6,7] and *hypermethylated-in-cancer (HIC)-1*[8] genes, are silenced by DNA hypermethylation in hepatocellular carcinomas (HCCs). DNA methyltransferase (DNMT) 1 expression is significantly higher even in noncancerous liver tissue showing chronic hepatitis or cirrhosis than in the normal liver tissue and is even higher in HCCs.[9,10] DNMT1 overexpression is also correlated with poorer tumor differentiation, portal vein involvement and intrahepatic metastasis of HCCs and poorer patient outcome.[11] On the other hand, overexpression of DNMT3b4, an inactive splice variant of DNMT3b, may lead to chromosomal instability through induction of DNA hypomethylation in pericentromeric satellite regions during hepatocarcinogenesis.[12]

Because aberrant DNA methylation is one of the earliest molecular events during hepatocarcinogenesis and also participates in malignant progression,[13,14] it may be possible to estimate the future risk of developing more malignant HCCs on the basis of DNA methylation status. However, only a few previous studies focusing on HCCs have used recently developed array-based technology for assessing genome-wide DNA methylation status,[15] and such studies have focused mainly on identification of tumor-related genes that are silenced by DNA methylation. DNA methylation profiles, which could become the optimum indicator for carcinogenetic risk estimation and prediction of patient outcome, should therefore be further explored during hepatocarcinogenesis using array-based approaches.

In this study, to clarify genome-wide DNA methylation profiles during multistage hepatocarcinogenesis, we performed bacterial artificial chromosome (BAC) array-based methylated CpG island amplification (BAMCA)[16–18] using a microarray of 4,361 BAC clones[19] in the normal liver tissue obtained from patients without HCCs, noncancerous liver tissue obtained from patients with HCCs, and in HCCs themselves.

Material and methods

Patients and tissue samples

As a learning cohort, 15 samples of the noncancerous liver tissue (N1 to N15) and 19 primary HCCs (T1 to T19) were obtained from surgically resected specimens from 16 patients who underwent partial hepatectomy at the National Cancer Center Hospital, Tokyo, Japan. The patients comprised 13 men and 3 women with a mean (±SD) age of 64.9 ± 7.4 years. Of these, 7 were positive for hepatitis B virus (HBV) surface antigen (HBs-Ag), 8 were positive for anti-hepatitis C virus (HCV) antibody (anti-HCV) and 1 was negative for both. Histological examination of the noncancerous liver tissue samples revealed findings compatible with chronic hepatitis in 5 and cirrhosis in 9 and no remarkable histological findings in 1.

Additional Supporting Information may be found in the online version of this article.

Grant sponsors: Ministry of Health, Labor and Welfare of Japan (Third Term Comprehensive 10-Year Strategy for Cancer Control and Cancer Research), New Energy and Industrial Technology Development Organization (NEDO), National Institute of Biomedical Innovation (NiBio) (Program for Promotion of Fundamental Studies in Health Sciences).

***Correspondence to:** Pathology Division, National Cancer Center Research Institute, 5-1-1 Tsukiji, Chuo-ku, Tokyo 104-0045, Japan. Fax: +81-3-3248-2463. E-mail: ykanai@ncc.go.jp

Received 3 February 2009; Accepted after revision 25 June 2009
DOI 10.1002/ijc.24708
Published online 30 June 2009 in Wiley InterScience (www.interscience.wiley.com).

For the comparison, 10 normal liver tissue samples (C1 to C10) showing no remarkable histological findings were also obtained from 10 patients without HCCs who were both HBs-Ag- and anti-HCV-negative. The patients comprised 7 men and 3 women with a mean age of 58.4 ± 9.7 years. Nine patients underwent partial hepatectomy for liver metastases of primary colon cancers, and 1 patient did so for liver metastases of gastrointestinal stromal tumor of the stomach.

In addition, for the comparison, 7 liver tissue samples (V1 to V7) were obtained from 7 patients who were positive for HBs-Ag or anti-HCV, but who had never developed HCCs. The patients comprised 4 men and 3 women with a mean age of 62.4 ± 5.2 years. Three patients underwent partial hepatectomy for liver metastases of primary colon or rectal cancers, and 1 patient did so for liver metastases of gastric cancer. Three patients underwent partial hepatectomy for cholangiocellular carcinomas.

As a validation cohort, 26 normal liver tissue samples (C11 to C36) showing no remarkable histological features were obtained from 26 patients without HCCs who were both HBs-Ag- and anti-HCV-negative. Twenty-four noncancerous liver tissue samples (N16 to N 39) and 25 primary HCCs (T20 to T44) were obtained from surgically resected specimens from 24 patients who underwent partial hepatectomy were added. The patients from whom C11 to C36 were obtained comprised 21 men and 5 women with a mean age of 59.9 ± 10.9 years. The patients with HCCs from whom N16 to N 39 and T20 to T44 were obtained comprised 22 men and 2 women with a mean age of 61.6 ± 11.4 years. Of the 24 patients with HCCs from whom N16 to N 39 and T20 to T44 were obtained, 5 were positive for HBs-Ag, 16 were positive for anti-HCV and 3 were negative for both. Histological examination of N16 to N 39 revealed findings compatible with chronic hepatitis and cirrhosis in 16 and 8 samples, respectively.

This study was approved by the Ethics Committee of the National Cancer Center, Tokyo, Japan.

BAMCA

High molecular weight DNA from fresh-frozen tissue samples was extracted using phenol-chloroform followed by dialysis. Because DNA methylation status is known to be organ specific, the reference DNA for analysis of the developmental stages of HCCs should be obtained from the liver and not from other organs or peripheral blood. Therefore, a mixture of normal liver tissue DNA obtained from 5 male patients (C37 to C41) and 5 female patients (C42 to C46) was used as a reference for analyses of male and female test DNA samples, respectively.

DNA methylation status was analyzed by BAMCA using a custom-made array (MCG Whole Genome Array-4500) harboring 4,361 BAC clones located throughout chromosomes 1 to 22 and X and Y,[19] as described previously.[16–18] Briefly, 5-μg aliquots of test or reference DNA were first digested with 100 units of methylation-sensitive restriction enzyme *Sma* I and subsequently with 20 units of methylation-insensitive *Xma* I. Adapters were ligated to *Xma* I-digested sticky ends, and polymerase chain reaction (PCR) was performed with an adapter primer set. Test and reference PCR products were labeled by random priming with Cy3- and Cy5-dCTP (GE Healthcare, Buckinghamshire, UK), respectively, and precipitated together with ethanol in the presence of Cot-I DNA. The mixture was applied to array slides and incubated at 43°C for 72 hr. Arrays were scanned with a GenePix Personal 4100A (Axon Instruments, Foster City, CA) and analyzed using GenePix Pro 5.0 imaging software (Axon Instruments) and Acue 2 software (Mitsui Knowledge Industry, Tokyo, Japan). The signal ratios were normalized in each sample to make the mean signal ratios of all BAC clones 1.0.

Statistics

Differences in the average number of BAC clones that showed DNA methylation alterations between groups of samples were analyzed using the Mann-Whitney *U* test or the Kruskal-Wallis test. Correlations between DNA methylation alterations in noncancerous liver tissue samples and the incidence of metachronous development and recurrence of HCCs were analyzed using the chi-squared test. Differences at $p < 0.05$ were considered significant. BAC clones whose signal ratios yielded by BAMCA were significantly different between groups of samples were identified by Wilcoxon test ($p < 0.01$). A support vector machine algorithm and a leave-one-out cross-validation were used to identify BAC clones by which the cumulative error rate for discrimination of sample groups became minimal. Two-dimensional hierarchical clustering analysis of noncancerous liver tissue samples and the BAC clones, and such analysis of HCCs and the BAC clones, were performed using the Expressionist software program (Gene Data, Basel, Switzerland). Survival curves of patient groups with HCCs were calculated by the Kaplan-Meier method, and the differences were compared by the log-rank test. The Cox proportional hazards multivariate model was used to examine the prognostic impact of DNA methylation status, histological differentiation, portal vein tumor thrombi, intrahepatic metastasis and multicentricity. Differences at $p < 0.05$ were considered significant.

Results

Genome-wide DNA methylation alterations during multistage hepatocarcinogenesis

Figures. 1*a* and 1*b* show examples of scanned array images and scattergrams of the signal ratios (test signal/reference signal), respectively, for normal liver tissue from a patient without HCC (Panel C), and both noncancerous liver tissue (Panel N) and cancerous tissue (Panel T) from a patient with HCC. In all normal liver tissue samples, the signal ratios of 97% of the BAC clones were between 0.67 and 1.5 (red bars in Fig. 1*b*). Therefore, in noncancerous liver tissue obtained from patients with HCCs and HCCs, DNA methylation status corresponding to a signal ratio of less than 0.67 and more than 1.5 was defined as DNA hypomethylation and DNA hypermethylation of each BAC clone compared with normal liver tissue, respectively.

In samples of noncancerous liver tissue obtained from patients with HCCs, many BAC clones showed DNA hypo- or hypermethylation (Panel N of Fig. 1*b*). In the learning cohort, all 9 patients (100%) showing DNA hypo- or hypermethylation on 70 or more than 70 BAC clones in their noncancerous liver tissue samples developed metachronous or recurrent HCCs after hepatectomy, whereas only 2 (30%) of the 6 patients showing DNA hypo- or hypermethylation on less than 70 BAC clones in their noncancerous liver tissue samples did so ($p = 0.0235$).

In HCCs themselves, more BAC clones showed DNA hypo- or hypermethylation, and the degree of DNA hypo- or hypermethylation, *i.e.*, deviation of the signal ratio from 0.67 or 1.5, was increased (Panel T of Fig. 1*b*) in comparison with noncancerous liver tissue obtained from patients with HCCs. The average numbers of BAC clones showing a signal ratio of less than 0.67 ($p = 0.0000063$) and more than 1.5 ($p = 0.00000052$) were increased significantly relative to normal liver tissue, to noncancerous liver tissue obtained from patients with HCCs, and to HCCs (Table I).

There were no significant differences in the number of BAC clones showing DNA hypo- or hypermethylation in samples of normal liver tissue obtained from male and female patients without HCCs (66.0 ± 30.1 and 98.7 ± 55.9, $p = 0.362$) and noncancerous liver tissue (111.2 ± 68.4 and 60.7 ± 46.9, $p = 0.279$) and cancerous tissue (521.5 ± 255.8 and 626.7 ± 329.0, $p = 0.539$) obtained from male and female patients with HCCs, respectively. Although there were no significant differences in the number of BAC clones showing DNA hypo- or hypermethylation between HBV- and HCV-positive patients with HCCs in both noncancerous liver tissue (108.3 ± 80.5 and 98.4 ± 60.0, $p = 1.000$) and cancerous tissue (475.6 ± 323.8 and 497.0 ± 247.8, $p = 0.689$), Wilcoxon test ($p < 0.01$) identified BAC clones in which DNA methylation status differed significantly between HBV- and

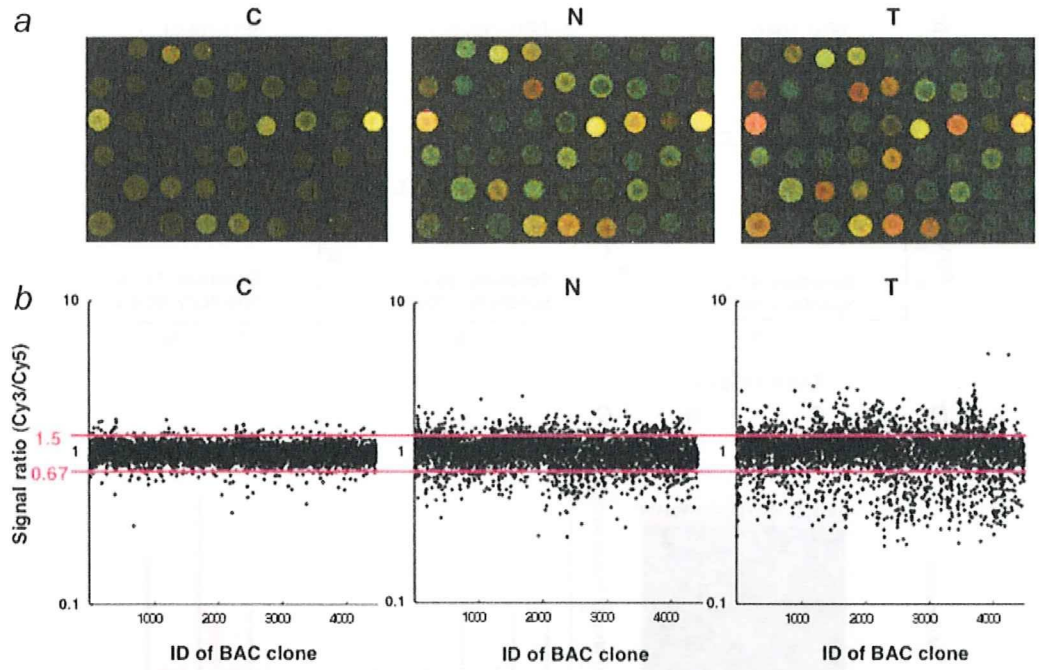

FIGURE 1 – Genome-wide DNA methylation alterations during multistage hepatocarcinogenesis. (*a*) Scanned array images yielded by BAMCA in normal liver tissue obtained from a patient without HCC (C) and noncancerous liver tissue (N) and cancerous tissue (T) obtained from a patient with HCC. (*b*) Scattergrams of the signal ratios yielded by BAMCA. In all C samples, the signal ratios of 97% of BAC clones were between 0.67 and 1.5 (red bars). In N and T, DNA methylation status corresponding to a signal ratio of less than 0.67 and more than 1.5 was defined as DNA hypomethylation and DNA hypermethylation on each BAC clone compared with C, respectively. Even in N, many BAC clones showed DNA hypo- or hypermethylation. In T, more BAC clones showed DNA hypo- or hypermethylation, and the degree of DNA hypo- or hypermethylation, *i.e.*, deviation of the signal ratio from 0.67 or 1.5 was increased in comparison with N.

TABLE I – GENOME-WIDE DNA METHYLATION ALTERATIONS DURING MULTISTAGE HEPATOCARCINOGENESIS

Tissue samples	Average number of BAC clones (mean ± SD)					
	Signal ratio <0.67 (DNA hypomethylation)	*p*	Signal ratio >1.5 (DNA hypermethylation)	*p*	Signal ratio <0.67 or >1.5(DNA hypo- or hypermethylation)	*p*
Normal liver tissue samples obtained from patient without HCCs (C, $n = 10$)	39.9 ± 20.8	0.0000063[1]	38.9 ± 24.9	0.00000052[1]	75.8 ± 39.3	0.00000061[1]
Noncancerous liver tissue samples obtained from patient with HCCs (N, $n = 15$)	61.2 ± 46.8	0.000102[2]	39.9 ± 27.3	0.0000026[2]	101.1 ± 66.5	0.0000065[2]
HCCs (T, $n = 19$)	278.9 ± 167.7	–	228.9 ± 125.7	–	507.8 ± 281.9	–

p values <0.05, which indicate significant differences.
[1]Kruskal-Wallis test among C, N and T.–[2]Mann-Whitney *U* test between N and T.

HCV-positive patients with HCCs in noncancerous liver tissue (18 BAC clones) and cancerous tissue (15 BAC clones), respectively.

DNA methylation profiles discriminating noncancerous liver tissue obtained from patients with HCCs from normal liver tissue

The above findings indicating accumulation of clinicopathologically significant genome-wide DNA methylation alterations in noncancerous liver tissue prompted us to estimate the degree of carcinogenetic risk based on DNA methylation profiles. Wilcoxon test ($p < 0.01$) revealed that the signal ratios of 512 BAC clones differed significantly between normal liver tissue samples and noncancerous liver tissue samples obtained from patients with HCCs. To omit potentially insignificant BAC clones associated only with inflammation and/or fibrosis and focus on BAC clones for which DNA methylation status was inherited by HCCs from the precancerous stage, we defined Groups I, II, III and IV. Group I: BAC clones in which the average signal ratio of noncancerous liver tissue obtained from patients with HCCs was higher than that of normal liver tissue and the average signal ratio of HCCs was even higher than that of noncancerous liver tissue obtained from patients with HCCs (41 BAC clones), Group II: BAC clones in which the average signal ratio of noncancerous liver tissue obtained from patients with HCCs was higher than that of normal liver tissue and the average signal ratio of HCCs did not differ from that of noncancerous liver tissue obtained from patients with HCCs (146 BAC clones), Group III: BAC clones in which the average signal ratio of noncancerous liver tissue obtained from patients with HCCs was lower than that of normal liver tissue and the average signal ratio of HCCs was even lower than that of noncancerous liver tissue obtained from patients with HCCs (40 BAC clones), and Group IV: BAC clones in which the average signal ratio of noncancerous liver tissue obtained from patients with HCCs was lower than that of normal liver tissue and the average

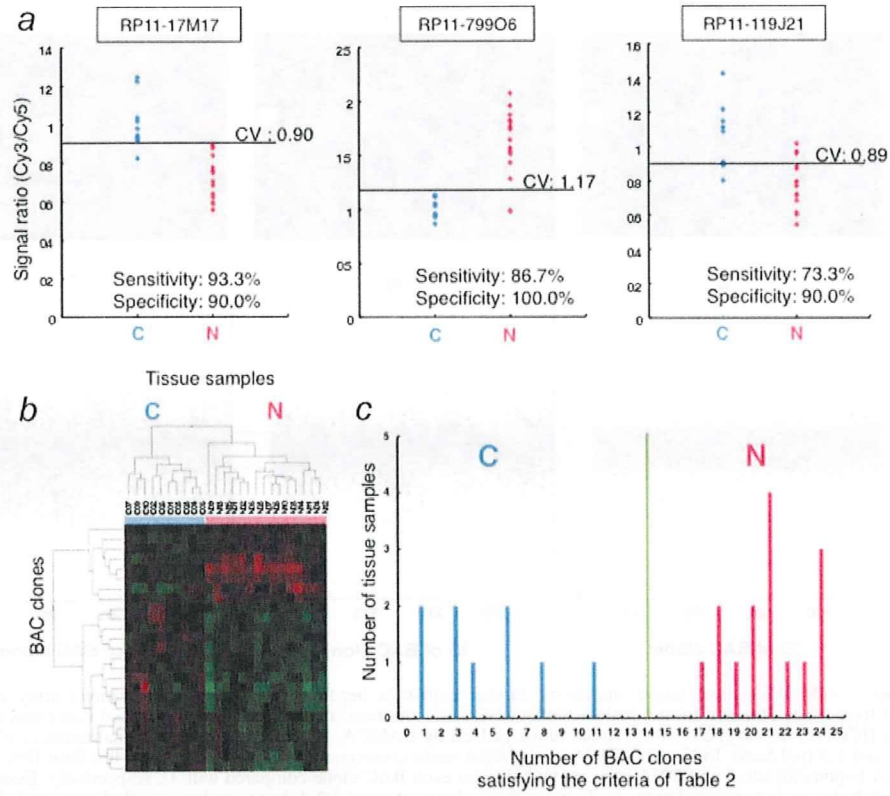

FIGURE 2 – DNA methylation profiles discriminating noncancerous liver tissue obtained from patients with HCCs from normal liver tissue. (*a*) Scattergrams of the signal ratios in normal liver tissue samples (C1 to C10) and noncancerous liver tissue samples obtained from patients with HCCs (N1 to N15) in the learning cohort on representative BAC clones, RP11-17M17, RP11-799O6 and RP11-119J21. Using the cutoff values (CV) described in each panel, noncancerous liver tissue samples obtained from patients with HCCs (N) in the learning cohort were discriminated from normal liver tissue samples (C) with sufficient sensitivity and specificity. (*b*) By 2-dimensional hierarchical clustering analysis using the 25 BAC clones selected by the process described in the Results section, normal liver tissue samples (C1 to C10) and noncancerous liver tissue samples obtained from patients with HCCs (N1 to N15) in the learning cohort were subclassified into the different subclasses without any error. The cluster trees for tissue samples and BAC clones are shown at the top and left of the panel, respectively. (*c*) Histogram showing the number of BAC clones satisfying the Table II criteria in samples C1 to C10 and N1 to N15. On the basis of this histogram, we established the following criteria: when the noncancerous liver tissue satisfied the criteria in Table II for 14 (green bar) or more than 14 BAC clones, it was judged to be at high risk of carcinogenesis.

signal ratio of HCCs did not differ from that of noncancerous liver tissue obtained from patients with HCCs (131 BAC clones). From the 512 BAC clones, 358 (Groups I, II, III and IV), in which the DNA methylation status was inherited by HCCs from noncancerous liver tissue, were selected. From the 358 BAC clones, the first 40 were identified by spot ranking analysis using the support vector machine algorithm for discrimination of noncancerous liver tissue obtained from patients with HCCs from normal liver tissue. Figure 2*a* shows scattergrams of the signal ratios in normal liver tissue samples and noncancerous liver tissue samples obtained from patients with HCCs on representative examples of the 40 BAC clones. Using the cutoff values described in each panel, noncancerous liver tissue obtained from patients with HCCs in the learning cohort was discriminated from normal liver tissue with sufficient sensitivity and specificity (Fig. 2*a*). From the 40 BAC clones, 25, for which such discrimination was performed with a sensitivity or specificity of 70% or more than 70%, were selected (Supporting Information Table S1). The cutoff values of the signal ratios for the 25 BAC clones, and their sensitivity and specificity, are shown in Table II. Two-dimensional hierarchical clustering analysis using the 25 BAC clones is shown in Figure 2*b*: 10 normal liver tissue samples (C1 to C10) and 15 noncancerous liver tissue samples obtained from patients with HCCs (N1 to N15) in the learning cohort were subclassified into different subclasses without any error. The number of BAC clones satisfying the criteria listed in Table II in noncancerous liver tissue samples showing chronic hepatitis (20.6 ± 1.8) was not significantly different from that showing cirrhosis (21.3 ± 2.4, $p = 0.542$) in the learning cohort.

A histogram showing the number of BAC clones satisfying the criteria listed in Table II for samples C1 to C10 and N1 to N15 is shown in Figure 2*c*. On the basis of this figure, we finally established the following criteria: when noncancerous liver tissue satisfied the criteria of Table II for 14 or more BAC clones (green bar in Fig. 2*c*), it was judged to be at high risk of carcinogenesis, and when noncancerous liver tissue satisfied the criteria of Table II for less than 14 BAC clones, it was judged not to be at high risk of carcinogenesis. Based on these criteria, both the sensitivity and specificity for diagnosis of noncancerous liver tissue samples obtained from patients with HCCs in the learning cohort as being at high risk of carcinogenesis were 100%.

To confirm these criteria, an additional 50 liver tissue samples were analyzed by BAMCA as a validation study (Supporting Information Figure S1). Twenty-three of 24 validation samples satisfying the criteria of Table II for 14 or more BAC clones were noncancerous liver tissue samples obtained from patients with HCCs (N16 to N36 and N38), and 24 of 26 validation samples satisfying the criteria of Table II for less than 14 BAC clones were normal

TABLE II – 25 BAC CLONES WHICH COULD DISCRIMINATE NONCANCEROUS LIVER TISSUES (N) FROM NORMAL LIVER TISSUES (C)

BAC clone ID	Location	Cutoff value	DNA methylation status[1]	Sensitivity (%)	Specificity (%)
RP11-104J13	1p35-1p36	1.01	C>N	93.3	70.0
RP11-52I2	1p34-1p35	1.00	C<N	80.0	60.0
RP11-29M22	1p11-1p12	1.11	C<N	86.7	90.0
RP11-21K1	2q37.2	1.00	C>N	86.7	70.0
RP11-109B15	5q33	1.04	C<N	66.7	90.0
RP11-88B24	6q26	0.95	C>N	80.0	70.0
RP11-112B7	7p13-7p14	1.00	C>N	80.0	70.0
RP11-48D21	8p11.2	1.00	C>N	80.0	90.0
RP11-120E20	11p15.4-11p15.5	0.90	C>N	73.3	100.0
RP11-334E6	11q23	1.00	C>N	86.7	80.0
RP11-17M17	11q25	0.90	C>N	93.3	90.0
RP11-319E16	12p13.32a	1.00	C>N	80.0	90.0
RP11-1100L3	12q13.13c-12q13.13d	1.04	C<N	86.7	80.0
RP11-799O6	12q13.3a-12q13.3b	1.17	C<N	86.7	100.0
RP11-119J21	12q24.33	0.89	C>N	73.3	90.0
RP11-332N6	14q11.2b	0.95	C>N	86.7	100.0
RP11-529E4	14q12c	1.00	C>N	93.3	50.0
RP11-89M4	16p13.2-16p13.3	1.20	C<N	86.7	100.0
RP11-215M5	15q15-15q21.1	1.00	C<N	86.7	70.0
RP11-348B12	19p13	1.00	C<N	80.0	80.0
RP11-134G22	20p11.2-20p12	1.01	C>N	80.0	90.0
RP11-328M17	22q13.2-22q13.33	0.93	C>N	86.7	100.0
RP11-354I12	22q13.31-22q13.33	1.00	C>N	93.3	80.0
RP11-55J11	22q13.2-22q13.33	1.00	C>N	80.0	70.0
RP11-480M11	Xq27.1-Xq28	0.90	C>N	80.0	90.0

[1]C>N, when the signal ratio was lower than the cutoff value, the tissue sample was considered to be at high risk for carcinogenesis; C<N, when the signal ratio was higher than the cutoff value, the tissue sample was considered to be at high risk for carcinogenesis.

liver tissue samples (C11 to C31, 33, 34 and 36). That is, our criteria enabled diagnosis of noncancerous liver tissue samples obtained from patients with HCCs in the validation set as being at high risk of carcinogenesis with a sensitivity of 95.8% and a specificity of 96.2%. The number of BAC clones satisfying the criteria listed in Table II in noncancerous liver tissue samples showing chronic hepatitis (17.6 ± 2.5) was not significantly different from that showing cirrhosis (19.4 ± 1.8, $p = 0.128$) in the validation cohort.

In addition, the average number of BAC clones satisfying the criteria in Table II was significantly lower in 7 samples of liver tissue obtained from patients who were infected with HBV or HCV, but who had never developed HCCs (V1 to V7, 13.14 ± 4.78), than that in N1 to N39 (19.21 ± 2.67, $p = 0.00419$).

Association of HCC DNA methylation profiles with patient outcome

To establish criteria for prognostication of patients with HCCs, in the learning cohort, 5 of 19 HCC samples obtained from patients who had survived more than 4 years after hepatectomy and 6 of 19 HCC samples from patients who had suffered recurrence within 6 months and died within a year after hepatectomy were defined as a favorable-outcome group and a poor-outcome group, respectively. Wilcoxon test ($p < 0.01$) revealed that the signal ratios of 41 BAC clones (Supporting Information Table S1) differed significantly between the favorable-outcome group ($n = 5$) and the poor-outcome group ($n = 6$). Figure 3*a* shows scattergrams of the signal ratios in samples from the favorable- and poor-outcome groups for representative examples of the 41 BAC clones. Using the cutoff values described in Figure 3*a* and Table III for the 41 BAC clones, samples from the poor-outcome group were discriminated from favorable-outcome group samples with sufficient sensitivity and specificity (Fig. 3*a* and Table III). Two-dimensional hierarchical clustering analysis using the 41 BAC clones is shown in Figure 3*b*: 5 HCCs in the favorable-outcome group and 6 HCCs in the poor-outcome group were subclassified into different subclasses without any error (Fig. 3*b*). A histogram showing the number of BAC clones satisfying the criteria in Table III is shown in Fig. 3*c*. In all 19 HCCs in the learning cohort, multivariate analysis revealed that satisfying the criteria in Table III for 32 or more BAC clones was a predictor of overall patient outcome and was independent of parameters that are already known to have prognostic impact,[20] such as histological differentiation, portal vein tumor thrombi, intrahepatic metastasis and multicentricity (Table IV).

To confirm these criteria, an additional 25 HCC samples were analyzed by BAMCA as a validation study, and then evaluated based on the criteria in Table III. All 44 HCCs were divided into 2 groups according to the number of BAC clones satisfying the criteria (32 or more BAC clones *vs.* less than 32 BAC clones). The period covered ranged from 11 to 3,413 days (mean, 1,349 days). The cancer-free and overall survival rates of patients with HCCs satisfying the criteria in Table III for 32 or more BAC clones was significantly lower than that of patients with HCCs satisfying the criteria in Table III for less than 32 BAC clones (Fig. 3*d*, $p = 0.000000002$ and $p = 0.0013$, respectively).

Discussion

Although many researchers in the field of cancer epigenetics use promoter arrays to identify the genes that are methylated in cancer cells,[21–23] we used a BAC array[19] in this study. The efficiency of identification of specific genes that are silenced by DNA methylations around the promoter regions and may become a target of therapy may be generally lower using the BAMCA approach than with conventional promoter array-based analysis. However, the promoter regions of specific genes are not the only target of DNA methylation alterations in human cancers. DNA methylation status in genomic regions not directly participating in gene silencing, such as the edges of CpG islands, may be altered at the precancerous stage before the alterations of the promoter regions themselves occur.[24] Moreover, aberrant DNA methylation of large regions of chromosomes, which are regulated in a coordinated manner in human cancers due to a process of long-range epigenetic silencing, has recently attracted attention.[25] BAMCA methods may be suitable for overviewing the DNA methylation status of individual large regions among all chromosomes and for

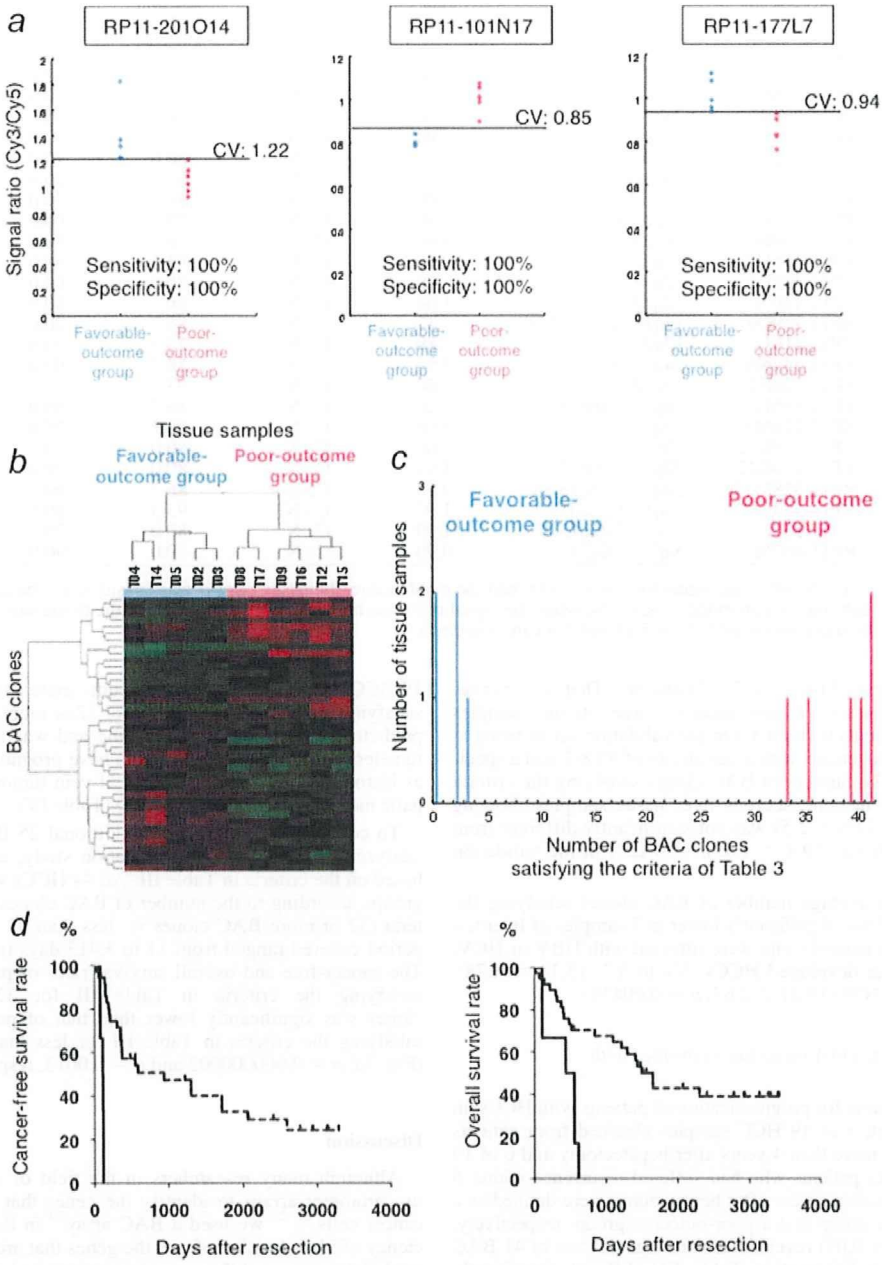

FIGURE 3 – DNA methylation profiles in HCCs associated with patient outcome. (*a*) Scattergrams of the signal ratios in HCCs from patients who survived more than 4 years after hepatectomy (favorable-outcome group, $n = 5$) and HCCs from patients who suffered recurrence within 6 months and died within a year after hepatectomy (poor-outcome group, $n = 6$) in the learning cohort for representative BAC clones, RP11-201O14, RP11-101N17 and RP11-177L7. Using the described cutoff values (CV), the poor-outcome group was discriminated from the favorable-outcome group with 100% sensitivity and specificity. (*b*) By 2-dimensional hierarchical clustering analysis using the 41 BAC clones selected by Wilcoxon test, HCCs in the favorable-outcome group and those in the poor-outcome group in the learning cohort were subclassified in the different subclasses without any error. The cluster trees for tissue samples and BAC clones are shown at the top and left of the panel, respectively. (*c*) Histogram showing the number of BAC clones satisfying the Table III criteria in HCCs of the favorable- and poor-outcome groups in the learning cohort. (*d*) Kaplan-Meier survival curves of all patients with HCCs (T1 to T44). The cancer-free (left panel, $p = 0.000000002$) and overall (right panel, $p = 0.0013$) survival rates of patients with HCCs satisfying the Table III criteria for 32 or more than 32 BAC clones (solid lines) were significantly lower than that of patients with HCCs satisfying the Table III criteria for less than 32 BAC clones (broken lines).

TABLE III – 41 BAC CLONES WHICH COULD DISCRIMINATE HCCS IN POOR-OUTCOME GROUP (P) FROM THOSE IN FAVORABLE-OUTCOME GROUP (F)

BAC clone ID	Location	Cutoff value	DNA methylation status[1]	Sensitivity (%)	Specificity (%)
RP11-89K16	1p35	1.50	F<P	83.3	100.0
RP11-201O14	1p34.3-1p36.13	1.22	F>P	100.0	100.0
RP11-156K6	1p31.1-1p31.3	1.15	F>P	100.0	80.0
RP11-553K8	1q31.2-1q31.3	1.16	F>P	100.0	100.0
RP11-89E10	1q31.3	0.91	F<P	100.0	100.0
RP11-180L21	2p16-2p21	1.29	F>P	100.0	80.0
RP11-90B13	2p14-2p15	1.13	F>P	83.3	100.0
RP11-449B19	2q11.2	0.75	F<P	100.0	80.0
RP11-30M1	2q32.3	1.10	F<P	100.0	100.0
RP11-89B13	2q32.3-2q33.1	1.11	F>P	83.3	80.0
RP11-255O19	3p24.3-3p25	1.08	F>P	100.0	100.0
RP11-421F9	3p24.2a	0.97	F>P	83.3	100.0
RP11-122D19	3p21.2	0.99	F<P	100.0	80.0
RP11-36K8	4q22	0.91	F>P	83.3	100.0
RP11-101N17	4q26	0.85	F<P	100.0	100.0
RP11-177L7	4q32	0.94	F>P	100.0	100.0
RP11-13O14	4q34-4q35	0.88	F<P	83.3	100.0
RP11-88H16	5p14	0.85	F<P	100.0	100.0
RP11-91G9	5q22-5q23	1.45	F<P	83.3	100.0
RP11-79K22	6q16	0.98	F<P	83.3	100.0
RP11-126B8	7q21.3	1.06	F>P	100.0	100.0
RP11-89P11	7q35	0.83	F>P	83.3	100.0
RP11-88N8	8q21.11d	1.02	F>P	100.0	100.0
RP11-85C21	9q33.3-9q34.2	0.95	F<P	83.3	100.0
RP11-714M16	10q26.11-10q26.3	1.00	F<P	100.0	100.0
RP11-48A2	10q26.2	0.69	F<P	100.0	80.0
RP11-206I1	11p11.2	1.20	F<P	100.0	100.0
RP11-35F11	11q12	1.30	F<P	100.0	80.0
RP11-158I9	11q23	1.04	F>P	83.3	100.0
RP11-74I8	12q13	1.13	F<P	100.0	100.0
RP11-167B4	16p13.3	0.97	F>P	83.3	100.0
RP11-368N21	16p11.2-16p12	1.10	F>P	83.3	100.0
RP11-303G21	16q12.1b	0.80	F>P	83.3	100.0
RP11-151M19	16q22	1.05	F>P	100.0	100.0
RP11-135N5	17p13.2	1.00	F>P	100.0	100.0
RP11-398A1	17q11.2d	1.00	F>P	100.0	100.0
RP11-15A1	19q13	1.08	F>P	83.3	100.0
RP11-697B10	19q13.3	0.90	F>P	83.3	100.0
RP11-79A3	19q13.3	1.05	F<P	100.0	100.0
RP11-29H19	20q12	1.00	F>P	100.0	100.0
RP11-36N5	22q11.2	1.15	F>P	83.3	100.0

[1]F>P, when the signal ratio was lower than the cutoff value, the tissue sample was considered to have been obtained from a patient with poor prognosis; F<P, when the signal ratio was higher than the cutoff value, the tissue sample was considered to have been obtained from a patient with poor prognosis.

identifying reproducible indicators for carcinogenetic risk estimation and prognostication. In fact, we have successfully obtained optimal indicators for carcinogenetic risk estimation and prognostication of renal cell carcinomas[26] and urothelial carcinomas (data will be published elsewhere) by BAMCA using the same array as that used in this study.

Our previous studies indicated that alterations of DNA methylation are one of the earliest events of multistage hepatocarcinogenesis and participate in malignant progression of HCCs.[5,7-14,27-29] However, since in previous studies we examined DNA methylation status on only a restricted number of CpG islands or chromosomal loci, it has not yet been clarified whether DNA methylation status on only restricted regions is simply altered at the precancerous stage, or whether genome-wide alterations of DNA methylation status have certain clinicopathological significance. As shown in Panel N of Figure 1*b*, genome-wide DNA methylation alterations (both hypo- and hypermethylation) were confirmed even in noncancerous liver tissue samples obtained from patients with HCCs. The number of BAC clones showing DNA methylation alterations and the degree of DNA methylation alterations were found to increase stepwise from the precancerous stage to the HCC stage (Fig. 1*b* and Table I). This study revealed that alterations of DNA methylation during multistage hepatocarcinogenesis occur in a genome-wide manner. Genome-wide DNA methylation alterations may participate in multistage hepatocarcinogenesis potentially through the induction of chromosomal instability and silencing of tumor-suppressor genes. DNA methylation alterations in noncancerous liver tissue were correlated with the future development of HCCs, suggesting that DNA methylation alterations at the precancerous stage may not occur randomly but are prone to further accumulation of genetic and epigenetic alterations.

Although mass vaccination against HBV has been initiated, this will not have a major impact for many years, as the age at presentation of HBV is older than 50 years mainly in Asia and Africa.[30] The spread of HCV in Japan that occurred in the 1950s and 1960s has resulted in a rapid increase in the incidence of HCC since 1980. In other countries including the United States, where HCV infection spread more recently, an increase in the incidence of HCC is imminent.[31] Although there were no significant differences in the number of BAC clones showing DNA hypo- or hypermethylation between HBV- and HCV-positive patients with HCCs, Wilcoxon test identified BAC clones in which DNA methylation status differed significantly between HBV- and HCV-positive patients with HCCs in both noncancerous liver tissue and cancerous tissue, suggesting that the HBV-related carcinogenetic

TABLE IV – MULTIVARIATE ANALYSIS OF CLINICOPATHOLOGICAL PARAMETERS AND DNA METHYLATION PROFILES ASSOCIATED WITH OVERALL OUTCOME IN PATIENTS WITH HCCS

Parameters	Hazard ratio (95% CI)	χ^2	p
Histological differentiation			
Well differentiated	1 (Reference)	0.031	0.8594
Moderately or poorly differentiated	0.817 (0.088-7.616)		
Portal vein tumor thrombi			
Negative	1 (Reference)	2.095	0.1478
Positive	4.474 (0.588-34.033)		
Intrahepatic metastasis[1]			
Negative	1 (Reference)	0.090	0.7647
Positive	1.248 (0.292-5.336)		
Multicentricity[1]			
Negative	1 (Reference)	1.499	0.2209
Positive	0.328 (0.055-1.955)		
The criteria of Table 3			
Satisfying for less than 32 BAC clones	1 (Reference)	4.997	0.0254
Satisfying for 32 or more BAC clones	4.466 (1.202-16.585)		

CI, confidence interval.
[1]In patients with multiple lesions, whether the lesions other than the main tumor from which tissue samples were obtained for this study were intrahepatic metastases of the main tumor or second primary lesions was judged by microscopic observation of hepatectomy specimens based on the previously described criteria.[35]

pathway may result in distinct DNA methylation profiles. These findings are in accordance with a previous report showing that HBV-related proteins can induce DNA methylation alterations.[32]

The effectiveness of surgical resection for HCC is limited, unless the disease is diagnosed early at the asymptomatic stage. Therefore, surveillance at the precancerous stage will become a priority. To reveal the baseline liver histology, microscopic examination of liver biopsy specimens is performed in patients with HBV or HCV infection prior to interferon therapy.[33,34] Therefore, carcinogenetic risk estimation using such liver biopsy specimens will be advantageous for close follow-up of patients who are at high risk of HCC development. Because even subtle alterations of DNA methylation profiles at the precancerous stage are stably preserved on DNA double strands by covalent bonds, they may be better indicators for risk estimation than mRNA and protein expression profiles that can be easily affected by the microenvironment of precursor cells.

The present genome-wide analysis revealed DNA methylation profiles that were able to discriminate noncancerous liver tissue obtained from patients with HCCs from normal liver tissue and diagnose it at high risk of HCC development in the learning set. The sensitivity and specificity in the validation set were 95.8 and 96.2%, respectively, and the criteria listed in Table II were validated. For carcinogenetic risk estimation using liver biopsy specimens obtained prior to interferon therapy, DNA methylation profiles actually associated with carcinogenesis should be discriminated from those associated with inflammation and/or fibrosis. Therefore, we first omitted potentially insignificant BAC clones associated only with inflammation and/or fibrosis and focused on BAC clones for which DNA methylation status was inherited by HCCs from the precancerous stage (Groups I, II, III and IV). In fact, it was confirmed that there were no significant differences in the number of BAC clones satisfying the criteria in Table II between noncancerous liver tissue samples showing chronic hepatitis and noncancerous liver tissue samples showing cirrhosis, not only in the learning set ($p = 0.542$) but also in the validation set ($p = 0.128$), indicating that our criteria were not associated with the degree of inflammation or fibrosis. In addition, the average numbers of BAC clones satisfying the criteria in Table II were significantly lower in liver tissue of patients without HCCs (V1 to V7) than in noncancerous liver tissue of patients with HCCs (N1 to N39), even though the patients from whom V1 to V7 were obtained were infected with HBV or HCV. Therefore, our criteria not only discriminate noncancerous liver tissue obtained from patients with HCCs from normal liver tissue but may also be applicable for classifying liver tissue obtained from patients who are followed up because of HBV or HCV infection, chronic hepatitis or cirrhosis into that which may generate HCCs and that which will not. Our criteria are applicable to both patients with chronic hepatitis and liver cirrhosis, although liver cirrhosis is known to show a more pronounced tendency to lead to HCC development than chronic hepatitis.[20] We intend to validate the reliability of such risk estimation prospectively using liver biopsy specimens obtained prior to interferon therapy from a large cohort of patients. On the basis of the present data, we now consider it justifiable to propose that clinicians can apply a portion of biopsy cores for this type of prospective study.

Because a sufficient quantity of good-quality DNA can be obtained from liver biopsy specimens, PCR-based analyses focusing on individual CpG sites are not always required. Although cut-off values should be modified for widely available standardized reference DNA, array-based analysis that overviews aberrant DNA methylation in each BAC region is immediately applicable to routine laboratory examinations. Moreover, because DNA methylation status of CpG sites is often regulated in a coordinated manner in each individual large region on chromosomes,[13,14,25] an overview of the DNA methylation tendency (hypo- or hypermethylation) in the whole BAC region can be a more reproducible diagnostic indicator than one focusing on individual CpG sites.

The present genome-wide analysis revealed DNA methylation profiles that were able to discriminate a poor-outcome group from a favorable-outcome group. Correlation between the DNA methylation profiles and both cancer-free and overall survival rates of patients with HCCs (Fig. 3*d*) validated the criteria in Table III. Prognostication based on our criteria may be promising for supportive use during follow-up after surgical resection, because multivariate analysis revealed that our criteria can predict overall patient outcome independently of parameters observed in hepatectomy specimens that are already known to have prognostic impact.[20] Such prognostication using liver biopsy specimens obtained before transarterial embolization, transarterial chemoembolization and radiofrequency ablation may be advantageous even to patients who undergo such therapies. The reliability of such prognostication needs to be validated again prospectively in surgically resected specimens or biopsy specimens.

References

1. Jones PA, Baylin SB. The fundamental role of epigenetic events in cancer. Nat Rev Genet 2002;3:415–28.
2. Gronbaek K, Hother C, Jones PA. Epigenetic changes in cancer. APMIS 2007;115:1039–59.
3. Eden A, Gaudet F, Waghmare A, Jaenisch R. Chromosomal instability and tumors promoted by DNA hypomethylation. Science 2003; 300:455.
4. Baylin SB, Ohm JE. Epigenetic gene silencing in cancer—a mechanism for early oncogenic pathway addiction? Nat Rev Cancer 2006;6:107–16.
5. Kanai Y, Ushijima S, Tsuda H, Sakamoto M, Sugimura T, Hirohashi S. Aberrant DNA methylation on chromosome 16 is an early event in hepatocarcinogenesis. Jpn J Cancer Res 1996;87: 1210–7.
6. Yoshiura K, Kanai Y, Ochiai A, Shimoyama Y, Sugimura T, Hirohashi S. Silencing of the E-cadherin invasion-suppressor gene by CpG methylation in human carcinomas. Proc Natl Acad Sci USA 1995;92:7416–9.
7. Kanai Y, Ushijima S, Hui AM, Ochiai A, Tsuda H, Sakamoto M, Hirohashi S. The E-cadherin gene is silenced by CpG methylation in human hepatocellular carcinomas. Int J Cancer 1997; 71:355–9.
8. Kanai Y, Hui AM, Sun L, Ushijima S, Sakamoto M, Tsuda H, Hirohashi S. DNA hypermethylation at the D17S5 locus and reduced HIC-1

mRNA expression are associated with hepatocarcinogenesis. Hepatology 1999;29:703–9.
9. Sun L, Hui AM, Kanai Y, Sakamoto M, Hirohashi S. Increased DNA methyltransferase expression is associated with an early stage of human hepatocarcinogenesis. Jpn J Cancer Res 1997;88:1165–70.
10. Saito Y, Kanai Y, Sakamoto M, Saito H, Ishii H, Hirohashi S. Expression of mRNA for DNA methyltransferases and methyl-CpG-binding proteins and DNA methylation status on CpG islands and pericentromeric satellite regions during human hepatocarcinogenesis. Hepatology 2001;33:561–8.
11. Saito Y, Kanai Y, Nakagawa T, Sakamoto M, Saito H, Ishii H, Hirohashi S. Increased protein expression of DNA methyltransferase (DNMT) 1 is significantly correlated with the malignant potential and poor prognosis of human hepatocellular carcinomas. Int J Cancer 2003;105:527–32.
12. Saito Y, Kanai Y, Sakamoto M, Saito H, Ishii H, Hirohashi S. Overexpression of a splice variant of DNA methyltransferase 3b. DNMT3b4, associated with DNA hypomethylation on pericentromeric satellite regions during human hepatocarcinogenesis. Proc Natl Acad Sci USA 2002;99:10060–5.
13. Kanai Y, Hirohashi S. Alterations of DNA methylation associated with abnormalities of DNA methyltransferases in human cancers during transition from a precancerous to a malignant state. Carcinogenesis 2007;28:2434–42.
14. Kanai Y. Alterations of DNA methylation and clinicopathological diversity of human cancers. Pathol Int 2008;58:544–58.
15. Gao W, Kondo Y, Shen L, Shimizu Y, Sano T, Yamao K, Natsume A, Goto Y, Ito M, Murakami H, Osada H, Zhang J, et al. Variable DNA methylation patterns associated with progression of disease in hepatocellular carcinomas. Carcinogenesis 2008; 29:1901–10.
16. Misawa A, Inoue J, Sugino Y, Hosoi H, Sugimoto T, Hosoda F, Ohki M, Imoto I, Inazawa J. Methylation-associated silencing of the nuclear receptor 1I2 gene in advanced-type neuroblastomas, identified by bacterial artificial chromosome array-based methylated CpG island amplification. Cancer Res 2005;65:10233–42.
17. Sugino Y, Misawa A, Inoue J, Kitagawa M, Hosoi H, Sugimoto T, Imoto I, Inazawa J. Epigenetic silencing of prostaglandin E receptor 2 (PTGER2) is associated with progression of neuroblastomas. Oncogene 2007;26:7401–13.
18. Tanaka K, Imoto I, Inoue J, Kozaki K, Tsuda H, Shimada Y, Aiko S, Yoshizumi Y, Iwai T, Kawano T, Inazawa J. Frequent methylation-associated silencing of a candidate tumor-suppressor. CRABP1, in esophageal squamous-cell carcinoma. Oncogene 2007;26:6456–68.
19. Inazawa J, Inoue J, Imoto I. Comparative genomic hybridization (CGH)-arrays pave the way for identification of novel cancer-related genes. Cancer Sci 2004;95:559–63.
20. Hirohashi S, Ishak KG, Kojiro M, Wanless IR, These ND, Tsukuma H, Blum HE, Deugnier Y, Puig PL, Fischer HP, Sakamoto M. Hepatocellular carcinoma. In: Hamilton SR, Altonen LA, eds. World Health Organization classification of tumours. Pathology and genetics. Tumours of the digestive system. Lyon: IARC Press, 2000. 159–72.
21. Estecio MR, Yan PS, Ibrahim AE, Tellez CS, Shen L, Huang TH, Issa JP. High-throughput methylation profiling by MCA coupled to CpG island microarray. Genome Res 2007;17:1529–36.
22. Jacinto FV, Ballestar E, Ropero S, Esteller M. Discovery of epigenetically silenced genes by methylated DNA immunoprecipitation in colon cancer cells. Cancer Res 2007;67:11481–6.
23. Nielander I, Bug S, Richter J, Giefing M, Martin-Subero JI, Siebert R. Combining array-based approaches for the identification of candidate tumor suppressor loci in mature lymphoid neoplasms. APMIS 2007;115:1107–34.
24. Maekita T, Nakazawa K, Mihara M, Nakajima T, Yanaoka K, Iguchi M, Arii K, Kaneda A, Tsukamoto T, Tatematsu M, Tamura G, Saito D, et al. High levels of aberrant DNA methylation in *Helicobacter pylori*-infected gastric mucosae and its possible association with gastric cancer risk. Clin Cancer Res 2006;12:989–95.
25. Frigola J, Song J, Stirzaker C, Hinshelwood RA, Peinado MA, Clark SJ. Epigenetic remodeling in colorectal cancer results in coordinate gene suppression across an entire chromosome band. Nat Genet 2006; 38:540–9.
26. Arai E, Ushijima S, Fujimoto H, Hosoda F, Shibata T, Kondo T, Yokoi S, Imoto I, Inazawa J, Hirohashi S, Kanai Y. Genome-wide DNA methylation profiles in both precancerous conditions and clear cell renal cell carcinomas are correlated with malignant potential and patient outcome. Carcinogenesis 2009;30:214–21.
27. Kanai Y, Ushijima S, Tsuda H, Sakamoto M, Hirohashi S. Aberrant DNA methylation precedes loss of heterozygosity on chromosome 16 in chronic hepatitis and liver cirrhosis. Cancer Lett 2000;148:73–80.
28. Kondo Y, Kanai Y, Sakamoto M, Mizokami M, Ueda R, Hirohashi S. Genetic instability and aberrant DNA methylation in chronic hepatitis and cirrhosis—A comprehensive study of loss of heterozygosity and microsatellite instability at 39 loci and DNA hypermethylation on 8 CpG islands in microdissected specimens from patients with hepatocellular carcinoma. Hepatology 2000;32:970–9.
29. Kanai Y, Saito Y, Ushijima S, Hirohashi S. Alterations in gene expression associated with the overexpression of a splice variant of DNA methyltransferase 3b, DNMT3b4, during human hepatocarcinogenesis. J Cancer Res Clin Oncol 2004;130:636–44.
30. Chang MH, Chen CJ, Lai MS, Hsu HM, Wu TC, Kong MS, Liang DC, Shau WY, Chen DS. Universal hepatitis B vaccination in Taiwan and the incidence of hepatocellular carcinoma in children. Taiwan Childhood Hepatoma Study Group. N Engl J Med 1997;336:1855–9.
31. Tanaka Y, Hanada K, Mizokami M, Yeo AE, Shih JW, Gojobori T, Alter HJ. Inaugural article: a comparison of the molecular clock of hepatitis C virus in the United States and Japan predicts that hepatocellular carcinoma incidence in the United States will increase over the next two decades. Proc Natl Acad Sci USA 2002;99:15584–9.
32. Park IY, Sohn BH, Yu E, Suh DJ, Chung YH, Lee JH, Surzycki SJ, Lee YI. Aberrant epigenetic modifications in hepatocarcinogenesis induced by hepatitis B virus X protein. Gastroenterology 2007; 132:1476–94.
33. Arase Y, Ikeda K, Suzuki F, Suzuki Y, Kobayashi M, Akuta N, Hosaka T, Sezaki H, Yatsuji H, Kawamura Y, Kobayashi M, Kumada H. Comparison of interferon and lamivudine treatment in Japanese patients with HBeAg positive chronic hepatitis B. J Med Virol 2007; 79:1286–92.
34. Yoshida H, Tateishi R, Arakawa Y, Sata M, Fujiyama S, Nishiguchi S, Ishibashi H, Yamada G, Yokosuka O, Shiratori Y, Omata M. Benefit of interferon therapy in hepatocellular carcinoma prevention for individual patients with chronic hepatitis C. Gut 2004;53:425–30.
35. Oikawa T, Ojima H, Yamasaki S, Takayama T, Hirohashi S, Sakamoto M. Multistep and multicentric development of hepatocellular carcinoma: histological analysis of 980 resected nodules. J Hepatol 2005;42:225–9.

GASTROENTEROLOGY 2009;136:2304–2315

BASIC—LIVER, PANCREAS, AND BILIARY TRACT

Disruption of *Dicer1* Induces Dysregulated Fetal Gene Expression and Promotes Hepatocarcinogenesis

SHIGEKI SEKINE,*,‡ REIKO OGAWA,* RIE ITO,* NOBUYOSHI HIRAOKA,* MICHAEL T. MCMANUS,‡ YAE KANAI,* and MATTHIAS HEBROK‡

*Pathology Division, National Cancer Center Research Institute, Tokyo, Japan; and ‡Diabetes Center, Department of Medicine, University of California San Francisco, San Francisco, California

BACKGROUND & AIMS: Growing evidence suggests that microRNAs coordinate various biological processes in the liver. We describe experiments to address the physiologic roles of these new regulators of gene expression in the liver that are as of yet largely undefined. **METHODS:** We disrupted Dicer, an enzyme essential for the processing of microRNAs, in hepatocytes using a conditional knockout mouse model to elucidate the consequences of loss of microRNAs. **RESULTS:** The conditional knockout mouse livers showed the efficient disruption of *Dicer1* at 3 weeks after birth. This resulted in prominent steatosis and the depletion of glycogen storage. *Dicer1*-deficient liver exhibited increased growth-promoting gene expression and the robust expression of fetal stage–specific genes. The consequence of Dicer elimination included both increased hepatocyte proliferation and overwhelming apoptosis. Over time, *Dicer1*-expressing wild-type hepatocytes that had escaped Cre-mediated recombination progressively repopulated the entire liver. Unexpectedly, however, two thirds of the mutant mice spontaneously developed hepatocellular carcinomas derived from residual *Dicer1*-deficient hepatocytes at 1 year of age. **CONCLUSIONS: Dicer and microRNAs have critical roles in hepatocyte survival, metabolism, developmental gene regulation, and tumor suppression in the liver. Loss of Dicer primarily impairs hepatocyte survival but can promote hepatocarcinogenesis in cooperation with additional oncogenic stimuli.**

Dicer, an endoribonuclease III type enzyme, cleaves premicroRNAs and double-stranded RNAs into mature microRNAs and short interfering RNAs. Previous studies have shown that the disruption of Dicer results in the loss of mature microRNAs, indicating that Dicer is necessary for microRNA processing.[1–3] While the exact mechanisms are still under investigation, the involvement of microRNAs in the coordination of many biological processes via the regulation of messenger RNA expression and translation has been well established. Growing evidence suggests a physiologic role of microRNAs in the liver. The down-regulation of mir-122, the most abundant microRNA in hepatocytes, resulted in the suppression of cholesterol biosynthesis and the treated mice became resistant to high-fat diet–induced steatosis.[4,5] Furthermore, Grimm et al reported that the injection of a high-titer hairpin RNA expression vector into mice resulted in fatal liver dysfunction and injury.[6] These mice showed impaired microRNA processing arising from oversaturation of exportin-5–dependent microRNA transport, and the results were interpreted to suggest that microRNAs are indispensable for proper liver function and hepatocyte survival.

In addition to the roles in the regulation of physiologic functions of the liver, microRNAs are likely involved in hepatocarcinogenesis. Many microRNAs show altered expression in hepatocellular carcinomas (HCCs),[7,8] and mir-122, which targets *CCNG1*, is frequently down-regulated in HCCs.[8] However, the mechanisms by which the altered microRNA expression contributes to hepatocarcinogenesis remain largely unclear.

To elucidate the role of Dicer and microRNAs in the liver, we generated hepatocyte-specific *Dicer1* knockout mice. Because Dicer is encoded by a single locus within the mouse genome, the disruption of the single *Dicer1* gene results in the loss of all microRNAs.[1–3,9] Our findings showed that Dicer is necessary for hepatocyte survival and proper metabolic regulation. Furthermore, a significant proportion of the knockout mice spontaneously developed HCCs, providing evidence for the tumor suppressive activity of *Dicer1*.

Abbreviation used in this paper: PCR, polymerase chain reaction.

0016-5085/09/$36.00
doi:10.1053/j.gastro.2009.02.067

Materials and Methods

Mice

Alb promoter-driven Cre recombinase transgenic mice (*Albumin-Cre* mice) and mice carrying the floxed allele of *Dicer1* (*Dicer1*$^{loxP/loxP}$ mice) have been previously described.[1,10] *Albumin-Cre* and *Dicer1*$^{loxP/loxP}$ mice were crossed to obtain hepatocyte-specific *Dicer1* knockout mice (*Albumin-Cre;Dicer1*$^{loxP/loxP}$ mice). *Dicer1*$^{loxP/loxP}$ littermates were used as controls throughout the experiment. The mice used in the present study were maintained in barrier facilities according to the protocols approved by the Committee on Animal Research of the University of California San Francisco and the Committee for Ethics in Animal Experimentation at the National Cancer Center, Japan.

Histologic Analysis

Formalin-fixed and paraffin-embedded sections were subjected to H&E staining. Immunohistochemistry was performed on either paraffin-embedded or frozen sections using the avidin-biotin complex method as previously described.[11] Primary antibodies used are listed in Supplementary Table 1. Oil red O staining was performed on frozen sections fixed with formalin. Periodic acid–Schiff staining was performed on frozen sections fixed with Carnoy's fixative. Electron microscopy analysis was performed using standard procedures.

In situ hybridization against mir-122 was performed on frozen sections using locked nucleic acid probe labeled with digoxigenin (Exiqon, Vedbeak, Denmark) as previously described.[12] The signal was visualized using NBT/BCIP as a chromogen.

Serum, Blood Glucose, and Liver Lipid Analysis

Blood samples were collected from the inferior vena cava at necropsy. The serum was then separated and subjected to analysis (IDEXX, MA and SRL, Tokyo, Japan). Mouse tail vein blood glucose levels were measured using a standard glucometer. A liver lipid analysis was performed using commercially available kits (Wako, Tokyo, Japan; and Eiken, Tokyo, Japan) following methanol-chloroform extraction.

Reverse-Transcription Polymerase Chain Reaction

Reverse-transcription reaction and conventional polymerase chain reaction (PCR) were performed using standard protocols. Quantitative PCRs were performed using SYBR Green PCR Master Mix (Applied Biosystems, Foster City, CA). The expression of liver genes was compared with the expression level of *Gusb,* as previously described.[11] The primer sequences are available upon request.

Northern Blotting

Total RNA was fractioned on a 15% polyacrylamide gel, transferred to nylon membrane, and hybridized to a radiolabeled oligonucleotide complementary to mir-122.[5] Ethidium bromide staining of 5S RNA served as a control.

Microarray Analysis

Total RNA was extracted from 3 control and 3 *Albumin-Cre;Dicer1*$^{loxP/loxP}$ mice. Complementary RNA synthesis and labeling was performed using GeneChip Two-Cycle Target Labeling and Control Reagent (Affymetrix, Santa Clara, CA). Gene expression profile was assessed by GeneChip Genome 430 2.0 Array (Affymetrix) following the manufacturer's protocol. Data analysis was performed on the NIA array analysis Web site.[13] Genes that showed more than 2-fold changes with a false discovery rate <0.05 were considered significantly altered. Gene Ontology analysis was performed using the DAVID functional annotation tool.[14] Overrepresented Gene Ontology terms for biological pathways among significantly altered genes were analyzed with default settings.

MicroRNA expression was also determined for the same set of RNA samples. Samples were labeled using miRCURY LNA microRNA Power Hy3/Hy5 Labeling Kit (Exiqon) and microRNA expression profiles were assessed by miRCURY LNA version 10.0 - hsa, mmu & rno (Exiqon). MicroRNAs that showed more than 2-fold changes with a false discovery rate <0.05 were considered significantly altered.

Western Blotting

Western blotting was performed as previously described.[11] Primary antibodies used are listed in Supplementary Table 1.

Statistical Analysis

The results are presented as mean ± SD. Statistical significance was determined by Student 2-tailed *t* test, with a *P* value of $<.05$ considered significant.

Results

Efficient Deletion of Dicer1 *in Young* Albumin-Cre;Dicer1$^{loxP/loxP}$ *Mouse Liver Is Followed by Repopulation With* Dicer1*-Expressing Hepatocytes*

Albumin-Cre transgenic mice and *Dicer1*$^{loxP/loxP}$ mice were crossed to achieve the hepatocyte-specific disruption of *Dicer1*.[1,10] *Albumin-Cre;Dicer1*$^{loxP/loxP}$ mice were born at the expected Mendelian ratio and survived to adulthood with no obvious growth phenotypes. An examination of *Albumin-Cre;Dicer1*$^{loxP/loxP}$ mice and their control littermates during young adulthood revealed apparent defects in liver morphology (Figure 1*A*). Three-week-old *Albumin-Cre;Dicer1*$^{loxP/loxP}$ mouse livers were homogenously pale

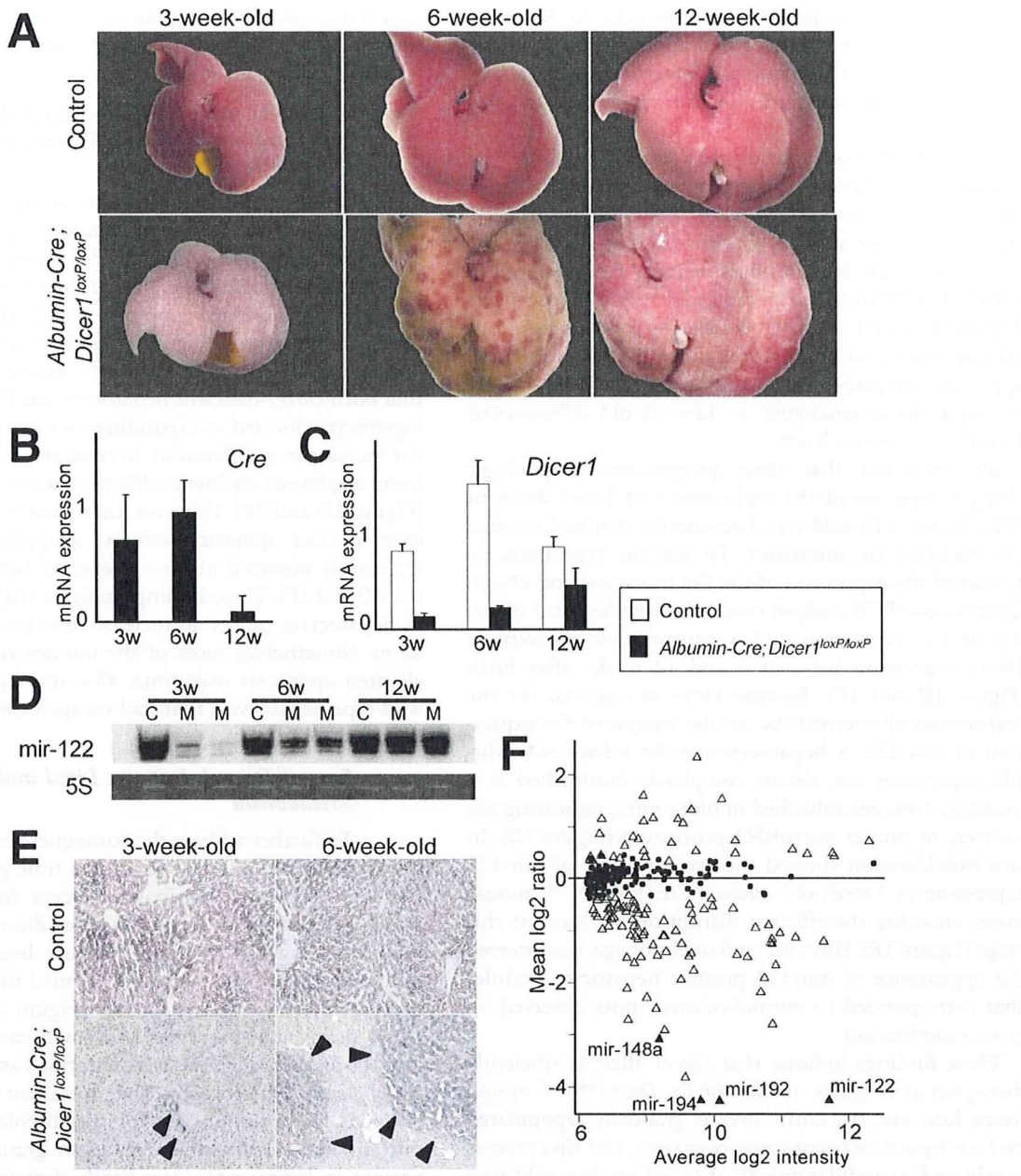

Figure 1. Efficient deletion of *Dicer1* in young *Albumin-Cre;Dicer1*$^{loxP/loxP}$ mouse liver and repopulation with *Dicer1*-expressing hepatocytes. (*A*) Gross morphology of control and *Albumin-Cre;Dicer1*$^{loxP/loxP}$ mouse livers at 3, 6, and 12 weeks after birth. At 3 weeks, the *Albumin-Cre;Dicer1*$^{loxP/loxP}$ mouse liver was pale compared with the control. At 6 weeks, the *Albumin-Cre;Dicer1*$^{loxP/loxP}$ liver had become yellowish, with the appearance of normal-colored spots. The normal-colored areas had expanded at 12 weeks. (*B*) Quantitative PCR analysis of *Cre* transgene expression in *Albumin-Cre;Dicer1*$^{loxP/loxP}$ mouse liver. (*C*) Quantitative PCR analysis of *Dicer1* expression. *Dicer1* expression recovered with age. (*D*) Northern blotting for mir-122. Ethidium bromide staining of 5S RNA was used as a loading control. C, control; M, mutant (*Albumin-Cre;Dicer1*$^{loxP/loxP}$). (*E*) In situ hybridization for mir-122. Mir-122 expression was determined in control and *Albumin-Cre;Dicer1*$^{loxP/loxP}$ mouse livers at 3 and 6 weeks of age. Livers from control mice showed diffuse expression of mir-122. Hepatocytes in the 3-week-old *Albumin-Cre;Dicer1*$^{loxP/loxP}$ mouse liver did not express mir-122 except for a few cells (*arrowheads*). Nodules of mir-122–positive hepatocytes (*arrowheads*) appeared in the 6-week-old *Albumin-Cre; Dicer1*$^{loxP/loxP}$ mouse liver. (*F*) Expression of microRNAs in 3-week-old *Albumin-Cre;Dicer1*$^{loxP/loxP}$ mouse livers. Relative expression levels of mouse microRNAs were determined in comparison with control mouse livers. MicroRNAs with significantly altered expression (false discovery rate <0.5) are represented by *open* and *black triangles*. Four previously reported liver-specific microRNAs are indicated by *black triangles*. *Black dots* indicate microRNAs without significant alteration.